

Applicability of remote sensing technologies for use in Ontario forest fire management protocols

by

Isabelle-Gabriele Hendel

A thesis submitted in partial fulfillment
of the requirements for the degree of
Masters of Science (M.Sc.) in Biology

The Faculty of Graduate Studies
Laurentian University
Sudbury, Ontario, Canada

© Isabelle-Gabriele Hendel, 2020

THESIS DEFENCE COMMITTEE/COMITÉ DE SOUTENANCE DE THÈSE
Laurentian Université/Université Laurentienne
Faculty of Graduate Studies/Faculté des études supérieures

Title of Thesis Titre de la thèse	Applicability of remote sensing technologies for use in Ontario forest fire management protocols	
Name of Candidate Nom du candidat	Hendel, Isabelle-Gabrielle	
Degree Diplôme	Master of Science	
Department/Program Département/Programme	Biology	Date of Defence Date de la soutenance August 20, 2020

APPROVED/APPROUVÉ

Thesis Examiners/Examineurs de thèse:

Dr. Gregory Ross
(Supervisor/Directeur de thèse)

Dr. David MacLean
(Committee member/Membre du comité)

Dr. Alexander Moise
(Committee member/Membre du comité)

Dr. Laura Chasmer
(External Examiner/Examineur externe)

Approved for the Faculty of Graduate Studies
Approuvé pour la Faculté des études supérieures
Dr. Serge Demers
Monsieur Serge Demers
Acting Dean, Faculty of Graduate Studies
Doyen intérimaire, Faculté des études supérieures

ACCESSIBILITY CLAUSE AND PERMISSION TO USE

I, **Isabelle-Gabrielle Hendel**, hereby grant to Laurentian University and/or its agents the non-exclusive license to archive and make accessible my thesis, dissertation, or project report in whole or in part in all forms of media, now or for the duration of my copyright ownership. I retain all other ownership rights to the copyright of the thesis, dissertation or project report. I also reserve the right to use in future works (such as articles or books) all or part of this thesis, dissertation, or project report. I further agree that permission for copying of this thesis in any manner, in whole or in part, for scholarly purposes may be granted by the professor or professors who supervised my thesis work or, in their absence, by the Head of the Department in which my thesis work was done. It is understood that any copying or publication or use of this thesis or parts thereof for financial gain shall not be allowed without my written permission. It is also understood that this copy is being made available in this form by the authority of the copyright owner solely for the purpose of private study and research and may not be copied or reproduced except as permitted by the copyright laws without written authority from the copyright owner.

Abstract:

The use of remote sensing in forest fire detection could allow earlier mitigation of active fires resulting in a significant decrease in fire related health effects. Infrared detection can provide more detailed and accurate information on fire size, spatial accuracy and temperature.

Hyperspectral sensors can allow the detection and earlier mitigation of high risk areas. Few studies have concentrated on the efficiency of multiple types of sensors such as infrared, hyperspectral and multispectral being used in combination. A literature review was done to highlight health effects on humans and the environment in order to determine the need for changes in current forest fire detection practices. The infrared portion of this research focused on sensors abilities to detect heat signatures and compared the specifications of each sensor with the others to ensure a cost-effective solution to current practices using off-the-shelf technologies.

The hyperspectral portion of this research focused on using vegetation indices to examine potential use of such sensors in the detection of high risk areas.

Keywords: Forest fire; health; infrared; hyperspectral; vegetation indices; fire fuels

Acknowledgements:

There are many people I would like to thank who made the completion of this M.Sc. thesis possible. Firstly, I would like to acknowledge my supervisor Dr. Gregory Ross for allowing me the opportunity to become a part of the NOSM research team. With his support I was able to become a better student and scientist. Thank you for helping me attain my goals even in these trying times. I am also grateful to my committee for their time and support.

I would also like to show my appreciation to the entire M.Sc. group at NOSM for listening to my endless ramblings about my large datasets and my several software's that never seemed to work properly. Danika and Hallie thank you for always being there for me and for making things fun even when they were stressful. Without you, NOSM would've been a lonely place. Natalie, thank you for keeping the research team going. Michelle, thank you for all that you did, without you Sarah and I would still be stuck.

I would like to dedicate a special paragraph to Sarah Lavallee, my first friend at NOSM. Sarah thank you for teaching me how to use the software's to the best of your ability, thank you for learning with me when we reached the capacity of your knowledge and for supporting me when I had to call in the big guns (calling the support numbers for each software) only to realize I would have to figure it out myself because even the companies did not know how to help. Thank you for always being available to answer questions and read drafts, for the endless rides and pen conversations. Without you I would never have been able to get to where I am. Also, Lunch o'clock would never have been the same. Hanna, thank you for making the summer the best part of my masters, Sarah and I needed that kind of refreshment in our lives.

Financial support from FedNor (Industry Canada), NOHFC (Province of Ontario) and MAG Aerospace Canada is gratefully acknowledged.

Finally, I would like to acknowledge my friends and family, who have always supported me and who might now officially believe I am a "Scientist". Emalie, your help with everything statistics related not only now, but throughout my entire academic career has been greatly appreciated. You're a pretty awesome big sister. Mom and Dad, thanks for feeding me and sitting on the couch while I taught you every single subject I've ever learnt. Miriam, Michel, Judy, Adam, Ericha, Paolo and Alexandar, thanks for believing I would actually finish one day. Last but certainly not least, thanks to my dogs and cats for being stress relievers and for being good while I was at school.

Table of Contents

<i>Abstract:</i>	<i>iii</i>
<i>Chapter 1: Introduction</i>	1
<i>Chapter 2: Thesis Hypothesis and objectives</i>	4
<i>Chapter 3: Remote sensing and the potential mitigation of forest fire related health effects</i>	5
<i>Chapter 4: Efficacy of remote sensing in early forest fire detection: a sensor comparison.....</i>	12
Abstract:.....	12
Résumé:	12
Introduction :	14
Materials and Methods:	20
Study site:	20
Sensors:	21
Aircraft:	24
Flight plans:	24
uTABI:	25
Hotspots:	26
uTABI:	26
Pro and Duo:.....	27
Temperature readings from the ground:	27
Resolution:	28
Spatial Accuracy:	28
Thermal accuracy:	28
Results:	28
uTABI:	28
Resolution:	28
Spatial accuracy:	29
Thermal accuracy:	31
Pro and Duo:	32
Resolution:	32
Thermal accuracy:	34
Discussion:	35
Resolution:	36
Spatial accuracy:	36
Thermal accuracy:	38
Conclusion:	41
Future research direction:	42
<i>Chapter 5: Pre-fire biofuel characterization and identification of high risk areas using hyperspectral remote sensing technologies</i>	44
Abstract:.....	44
Résumé:	44
Introduction.....	46

Materials and Methods:	50
<i>Study 1:</i>	50
Selection of Datasets:	50
Sensor:	52
Analysis:	53
Indices:	53
<i>Study 2:</i>	55
Selection of datasets:	55
Sensors:	59
Analysis:	64
Indices:	64
Results:	65
<i>Study 1:</i>	65
Forest health (FH):	65
Normalized Difference Vegetation Index (NDVI):	65
Plant Senescence Reflectance Index (PSRI):	66
Weather:	66
FH:	66
NDVI:	66
PSRI:	67
<i>Study 2:</i>	67
Cedar Fire:	67
Rim Fire:	67
King Fire:	68
Mendocino Fire Complex:	68
Discussion:	68
<i>Study 1:</i>	69
Forest health (FH):	69
Normalized Difference Vegetation Index (NDVI):	69
Plant Senescence Reflectance Index (PSRI):	69
Weather:	69
Overall trends:	70
<i>Study 2:</i>	71
Cedar Fire and Mendocino Fire Complex:	71
Rim Fire and King Fire:	72
Overall Trends:	72
Conclusion:	75
<i>Future research:</i>	76
Chapter 6: Conclusion	78
References:	80

List of Tables:

Chapter 4: Efficacy of remote sensing in early forest fire detection: a sensor comparison

Table 1. List of sensors and their specifications	30
Table 2. List of heaters and their coordinates	27
Table 3. Number of high temperature pixels associated to each heater per trial.	42

Chapter 5: Pre-fire biofuel characterization and identification of high risk areas using hyperspectral remote sensing technologies **tab**

Table 1. EO-1 Hyperion dataset information.....	66
Table 2. AVIRIS dataset information	67
Table 3. Landsat 7 dataset information.....	68
Table 4. Landsat 8 Mendocino Fire Complex dataset information before fire.....	69
Table 5. Landsat 8 Mendocino Fire Complex dataset information after fire.....	69
Table 6. Mean humidity %.....	74
Table 7. Mean index values inside and outside of burn scar areas for Cedar Fire, Mendocino Fire Complex, King Fire and Rim Fire	75

List of Figures:

Chapter 4: Efficacy of remote sensing in early forest fire detection: a sensor comparison

Figure 1. Demonstrates a satellite image of French River/Alban aerodrome (Google Maps, 2019). Runway 1 runs parallel to highway 607. Runway 2 runs approximately at a 90° angle to Runway 1.	28
Figure 2. Demonstrates heater placement and temperature plan. A represents the heater set up on June 21 st 2019, this is the set up for the uTABI data. B represents the heater set up on August 15 th 2019, this is the set up for the Duo Pro R and Duo R. Each point on the image represents a heater. Heaters 1 to 5 are displayed from right to left.	26
Figure 3. Demonstrates the relationship between ground sampling distance (GSD) in meters and altitude in meters for ITRES uTABI. [$r(5)=1$, $p<.001$, $R^2=1$].	29
Figure 4. Demonstrates the relationship between average spatial variance in meters and altitude in meters for ITRES uTABI data. [$r(5)=.98$, $p<.001$, $R^2=0.9596$].	30
Figure 5. Demonstrates the relationship between diameter in meters and altitude in meters for ITRES uTABI data. [$r(5)=.98$, $p<.001$, $R^2=0.9595$].	31
Figure 6. Demonstrates the aerial infrared view of hotspots from FLIR Duo Pro R. A1 represents heaters 1 and 2 from top to bottom at 200 ft AGL. A2 represents heaters 3, 4 and 5 from top to bottom at 200 ft AGL. B represents heaters 1 to 5 from bottom to top at 400 ft AGL. C represents heaters 2 to 5 from top to bottom at 1000 ft AGL. D represents heaters 2 to 5 from top to bottom at 2000 ft AGL.	33
Figure 7. Demonstrates the aerial infrared view of hotspots from FLIR DUO R. All photos represent heaters 1 to 5 from top to bottom. Heater 1 is out in all of the images of this set. A represents the infrared view from 200 ft AGL. B represents the infrared view from 400 ft AGL. C1 represents the infrared view from 1000 ft AGL. C2 represents the RGB view from 1000 ft AGL, the arrows demonstrate the placement of the heaters. D1 represents the infrared view from 2000 ft AGL. D2 represents the RGB view from 2000 ft AGL.	41

Chapter 5: Pre-fire biofuel characterization and identification of high risk areas using hyperspectral remote sensing technologies

Figure 1. Daisy Lake Uplands Provincial Park flight line, Sudbury, Ontario, Canada. The grey area represents the area from which data was collected.	58
Figure 2. NDVI images of Daisy Lake demonstrating the overlapping data that was run through all vegetation indices. A represents data acquired June 20 th . B represents data acquired July 3 rd . C represents data acquired July 8 th . D represents data acquired August 14 th	59
Figure 3. This figure represents the datasets used for study 2. The darker inner colour represents the area defined as inside. The lighter area represents the area defined as outside. A represents the data used for Cedar Fire. B represents the data used for Rim Fire. C represents the data used for King Fire. D represents the data used for Mendocino Fire Complex.	62

Chapter 1: Introduction

On October 4th, 1957, the Soviet Union successfully launched the world's first satellite, Sputnik (Dickson, 2001). In response, the United States attempted to launch the Naval Research Lab's Vanguard project which, exploded and became a nation-wide embarrassment (Nille & Lishick, 2003). Soon after this failed launch, the United States pooled resources and built a four-stage rocket and on January 31st 1958, Explorer 1 became the first successfully launched U.S. satellite (McDonald & Naugle, 2008). This officially started the "Space Race" and from this scientific research, the world of remote sensing was born.

Remote sensing is defined as the acquisition of information about an object or phenomenon without coming into contact with the area being studied (Campbell & Wynne, 2011). This information comes in the form of a special class of imagery that allows an overhead perspective of the area in question. This includes aerial photographs which can be taken from airplanes, satellites and Unmanned Aerial Vehicles (UAV), such as the data from this research, as well as from a number of other methods. These datasets have special properties such as the detection of various forms of radiation that allow us to better study the earth's surface. These remote sensing technologies have been and continue to be increasingly applied worldwide in areas such as resource exploration and development because they allow us to determine patterns and relationships between features that otherwise seem independent (Campbell & Wynne, 2011; Lo, 1986).

There are two types of remote sensing technologies, active and passive. Active sensors transmit energy to illuminate the target, then receive a portion of the energy scattered back as a reflection and are then able to form images of the surface of the area in question (Campbell &

Wynne, 2011). This involves the use of a transmitter which transmits microwave energy at a given frequency. The reflected energy is accepted by a receiver and is then filtered or amplified as required. Finally a recorder allows for the signal to be recorded and/or displayed as an image. Passive technologies detect variations in solar illumination and measure radiation that is emitted, reflected or absorbed from the target (Campbell & Wynne, 2011; Njoku & Entekhabi, 1996). RADAR and LiDAR technologies are considered active, while infrared, radiometers and film photography are considered passive (Tyo *et al*, 2006).

Thus far, the application of remote sensing technologies in forest fire management has been used in post-fire assessments however, it has been used less often for operational fire management coincident with burn . The literature seems to represent more research on the use of remote sensing post-fire in comparison to pre- and peri-fire. Passive technologies such as infrared sensors have mostly been used as an addition to other forms of passive sensors such as red-green-blue (RGB) sensors, in an effort to reduce false positives when these color sensors are being utilized in the field for smoke detection (Arrue *et al*, 2000). The use of active remote sensing technologies has concentrated on fuel type determination and quantification as well as in the determination of fire severity and post-fire recovery of vegetation (Joseph *et al*, 2011).

In this thesis, several studies were completed with the objective of determining the applicability of both passive and active remote sensing technologies for use in forest fire management protocols for the province of Ontario. To begin, the health impacts of forest fires were researched in order to establish a better understanding of the overall needs and implications that the introduction of remote sensing technologies could have on both the health of the environment and of humans. Next, the efficacy of several infrared sensors were examined in order to determine which sensors could be the most beneficial additions to current practices.

Finally, the use of hyperspectral technology in pre-fire biofuel characterization was examined in order to compare the applicability of this form of technology to previously explored multispectral technologies in the identification of areas at high-risk.

Chapter 2: Thesis Hypothesis and objectives

Hypothesis: Remote sensing technologies will be beneficial as an addition to forest detection practices.

Objectives:

- 1) Evaluate the impact of forest fires on the health of the environment and humans (Chapter 3).
- 2) Determine the use of infrared remote sensing as an alternative or additional method to current forest fire detection and prevention protocols (Chapter 4)
- 3) Assess the applicability of hyperspectral remote sensing in pre-fire vegetation analysis and risk management (Chapter 5).

Chapter 3: Remote sensing and the potential mitigation of forest fire related health effects

Hotspot detection is an important part of forest fire prevention, monitoring and maintenance as it allows initial data on location and fire size. The goal is to prevent injury and death to humans as well as to reduce secondary health hazards (from indirect contact). Protecting and monitoring environmental effects as well as reducing economic losses are also priorities (MNR, 2017). A literature review was done in order to explore the topic of health impacts of forest fires on both humans and the environment. Firstly, physical impacts on human health from fires were explored. This included impacts from direct contact, combustion and air pollution. Secondly, post-fire implications on ecosystems were examined.

When referring to fires in general it is clear that the majority of fatalities do not result from burns but rather from smoke inhalation (Stefanidou et al, 2008). For forest fires, the ecosystem's physical and chemical compositions are variable and the severity of smoke toxicity also varies accordingly (Stefanidou et al, 2008). Symptoms of acute smoke exposure may include burning eyes and tearing, runny nose and a sore throat (Fowler, 2003). More serious symptoms can include reduced pulmonary function, chronic obstructive pulmonary disease (COPD), asthma, heart disease, rhinitis and other respiratory and heart problems (Liu et al, 2016).

Smoke is comprised of a mixture of airborne solids, liquid particulates as well as gases, all of which are modified when they undergo vaporization and thermal decomposition (Nelson, 1987). The components present in smoke depend on the specific materials involved in the combustion (Liu et al, 2016). Smoke from vegetation fires usually contains carbon, oxygen and hydrogen which make up the combustion conditions. When burned completely, carbon is transformed into

carbon dioxide and water (Stefanidou et al, 2008). However, combustion conditions are rarely able to attain complete combustion meaning that the carbon is transformed into carbon monoxide (Stefanidou et al, 2008). Carbon monoxide can cause tissue hypoxia leading to the death of tissues because it starves organs of oxygen by affecting the function of hemoglobin (Naeher et al., 2007).

High particulate matter (PM) has also been correlated with health effects in humans caused by forest fires (Rittmaster et al, 2006). Fine particulate matter, defined as particulate matter with a diameter smaller than $2.5\text{ }\mu\text{m}$ ($\text{PM}_{2.5}$) in particular has been shown to have significant effects on human health (Haikerwal et al, 2009). Furthermore, atmospheric emissions from forest fires are known to impact air quality and therefore, human health (Stefanidou et al, 2008). One study found that PM levels associated with forest fires are 10 times more damaging to the alveolar macrophages than PM collected at an equal dosage under normal conditions (Wegesser et al, 2009). Furthermore, the number of findings related to this subject are limited due to the lack of proper measurement tools in this field of research (Fowler, 2003). Although it is clear that forest fire emissions of $\text{PM}_{2.5}$ and other particulate matter show important health related effects, it is therefore difficult to quantify PM trends. This is because of the sporadic nature of forest fires as well as the lack of technological resources (Jaffe et al, 2008).

Although the current 24 hour standards for PM_{10} (with a diameter of $10\text{ }\mu\text{m}$) established by the National Ambient Air Quality Standards (NAAQS) is of $150\text{ }\mu\text{g}/\text{m}^3$, one study done in Australia found that when PM_{10} levels exceed $40\text{ }\mu\text{g}/\text{m}^3$ hospital admissions for asthma increase rapidly (NAAQS, 2016; Bowman & Johnston, 2005).

Although fine particulate matter is the main constituent responsible for medical problems in relation to forest fire smoke inhalation, other components also play a role in the effect on human

health (WHO, 1999). Polycyclic aromatic hydrocarbons or PAHs are organic compounds which can be carcinogenic, for example benzopyrene. Formaldehyde may also be a component released from fires, as well as other aldehydes such as acrolein which produces irritation of mucous membranes and can cause pulmonary lesions. Other components such as free radicals can react with human tissues and create negative outcomes for those exposed. Furthermore, radionuclides such as iodine-129, chlorine-36, as well as cesium-137 can be released into the atmosphere, soil or water, and these radionuclides are all known carcinogens (Naeher et al., 2007; Miranda & Borrego, 2005; McDonald et al., 2000; Malilay, 1999).

Forest and bush fire smoke has been studied for many years and has been known to contain high levels of polychlorinated dibenzo-*p*-dioxins (PCDDs) (McMahon & Bush, 1992).

PCDDs, commonly known as dioxins, are thought to be an anthropogenically originated member of the chemical family polyhalogenated aromatics (Safe, 1986). The effects of PCDDs have been well studied in animals and are dependent on the age, sex and species of the animal subjected to the toxins as well as on the strain and dosage of the toxin itself (Safe, 1986). The majority of studies on PCDDs use non-human animal models and involve high-dose oral exposure (Mukerjee, 2011). No inhalation exposure data is available in the literature (Mukerjee, 2011). In humans, PCDDs have been confirmed as a cause for developmental defects in breast-fed children's teeth and thus the effects of the inhalation of PCDDs is thought to be quite important and multigenerational (Alaluusua et al, 1996).

Recent research has shown that cardiac problems are also associated with smoke inhalation (Liu et al, 2016). One study found evidence that the effect of smoke inhalation can also be seen in the reduction of red blood cell levels as well as in the destruction of cellular membranes indicated by the diminishment of macrophage activity and in the elevation of albumin and lactose

dehydrogenase levels (Larson & Koenig, 1994). Another study conducted in the 2000's, demonstrated an increase in white blood cell count as a result of forest fire smoke inhalation and determined that the increase was being caused by polymorphonuclear leukocyte precursors from the bone marrow (Tan et al, 2000). However, as previously mentioned, effects of smoke inhalation are dependent on the composition of the smoke as well as on age and pre-existing conditions which all influence the onset and severity of symptoms.

One such association has been found in a study conducted in the late 2000's where their findings demonstrate the susceptibility of different age groups to the effects of smoke inhalation (Delfino et al, 2009). This study found that the strongest associations between $PM_{2.5}$ and hospital admissions were in people over 65 years of age (with a 10% increase per $10 \mu g/m^3$ $PM_{2.5}$) and under 5 years of age (with an 8% increase per $10 \mu g/m^3$ $PM_{2.5}$) (Delfino et al, 2009). The conclusions drawn from these findings are that children are more susceptible because of their continuing airway development and that the elderly are the most susceptible because they have an increased amount of pre-existing conditions in comparison with younger people (Langmann et al, 2009; Stefanidou et al, 2008; Dokas et al, 2007).

One recent topic in terms of the effect of forest fires on human health is the idea of urban components making their way into the smoke composition. As previously mentioned, when a fire expands outwards and reaches urbanized land such as fields, landfills as well as city limits, burning of the materials in these areas releases components that can be hazardous to humans (Statheropoulos & Karma, 2007). This is a result of the extension in burning area materials such as plastics, pesticides, fungicides, fertilizers etc. which can also be burned and be added to the natural smoke components (Stefanidou et al, 2008). The components that originate from sources other than natural forest fuels can even mix with urban or industrial pollutants and create

secondary products which can result in both short and long term health effects in humans, especially firefighters (Statheropoulos & Karma, 2007). An example of man made compounds which may lead to increases in toxic by-products are herbicides. Contact with herbicides by workers such as firefighters as well as the people responsible for prescribed burnings have been labelled insignificant with lab findings but have not been a vast topic of field research, therefore the effects of these manmade products during wildland fires is not well documented and could be more significant than previously thought (McMahon & Bush, 1992).

Human health is directly impacted by the health of the environment around us. The health of the environment itself is also an area of interest in forest fire research. On major environmental impact is the emission of carbon from forest fires. Carbon emissions due to forest fires are estimated to average 27 Tg carbon per year for 1959-1999 in Canada this is equivalent to an average of 18% (2-75%) of carbon dioxide emissions (Amiro et al, 2001). This is very close to the average yearly carbon emissions from conventional oil for the same years which is equivalent to 29.8 Tg carbon per year meaning that the impact is great (Environment and Climate Change Canada, 2017). Post fire effects can also cause additional impacts on carbon emissions. Forest fire smoke not only affects humans but also our environment as it is a source of reactive organic substances which can react with urban or industrial pollutants to produce secondary substances such as O_3 (Hogue, 2005). These substances may cause additive or synergistic effects (Dokas et al, 2007). Furthermore, smoke can effectively decrease visibility by hazing caused by water vapor from fires condensing onto fine particles as well as by scattering light with fine soot particles (Statheropoulos & Goldammer, 2007). Decreased visibility means traditional fire monitoring may become more difficult or even impossible. In addition, the particles emitted by forest fires can affect cloud properties as well as precipitation by acting as cloud condensation

nuclei thereby further decreasing visibility from aerial detection (Vestin et al, 2007; Lin et al, 2006). The emissions from most fires are kept within 5 km in the atmospheric boundary however, depending on conditions the emissions could extend to the troposphere or even to the lower stratosphere, enhancing the lifetime of air pollutants (Langmann et al, 2009). Fire emissions are therefore becoming a global concern (Simoneit, 2002).

Additionally, forest fires can affect soil and water quality. Soil and water properties can be affected in many different ways including physical, chemical, mineralogical and biological. The results are dependent on the severity of the fire as characterized by both peak of temperatures as well as duration of the fire (Certini, 2005).

Fires classified as low to moderate, such as prescribed burnings promote revegetation of dominant species by removing competing plants (Certini, 2005). These prescribed burnings enable nutrient cycling by making nutrients available for new vegetation and by increasing pH levels. In the case of low to moderate fires no irreversible ecological changes occur. Severe fires such as wildland fires do create irreversible ecological changes. These fires cause the removal of significant amounts of organic material as well as a deterioration in the structure, nutrient load, as well as microbial and invertebrate content in soils (Certini, 2005). The result of severe burnings can also cause increased erosion due to the lack of contact of precipitation with vegetation that would normally slow it. The effects of fires on erosion are mainly determined by the amount of forest floor organic matter burned and the creation of water repellant conditions. This causes problems with sediment leaching as well as the leaching of ashes into the soil and eventually into water (Pannkuk & Robichaud, 2003). For example, one study found that the leaching of organic or particulate-bound mercury into waterways is facilitated after a fire (Burke et al, 2010).

The impacts of forest fires are endless, the loss of thousands of hectares, people and animals are just the beginning of the losses incurred (Bonazountas et al, 2007). Goods are lost, soil erosion occurs as the natural ecosystem ordinarily uses the presence of vegetation in order to control water runoff and with the burned vegetation erosion and compaction take place (Stokes et al, 2014; Bonazountas et al, 2007). Furthermore, the degradation of water quality and changes in hydrology are also provoked by the lack of interception of vegetation and by the compaction caused by erosion which together prevent the soaking in of rainwater which would ordinarily become a part of the underground water table. The loss of these and other ecological services is incredible (Stokes et al, 2014; Bonazountas et al, 2007).

The implementation of new technologies into current forest fire protocols could limit the health related effects to both humans and the environment by offering faster and more accurate information not only on fires but on areas at high risk. This would allow us to better understand the implications of fires on ecosystem function over short to long time scales as well as how this affects humans and ecosystem services. If this information could be acquired sooner, the health effects associated to forest fires could be better mitigated.

Chapter 4: Efficacy of remote sensing in early forest fire detection: a sensor comparison

Abstract:

The quantity and severity of forest fires is increasing on a yearly basis and current forest fire detection protocols are lacking. The objective of this research was to determine what technologies could be used to improve current forest fire detection methodologies.

Although human observation provides a wealth of information on the presence and size of fires, remote sensing technologies can provide increasingly more detailed, rapid, accurate and reliable information. Thus, the cost efficiency, thermal accuracy, spatial accuracy, range and resolution of three different thermal sensors were analysed. Our findings demonstrate that the incorporation of this form of technology in Ontario protocols would be beneficial and that limitations exist for each sensor depending on altitude. Our results indicate that the most affordable off-the-shelf addition to current forest fire detection protocols in Ontario would be the FLIR Duo Pro R.

Résumé:

La quantité et gravité de feux de forêts augmente à chaque année et les protocoles en place couramment ne sont pas appropriés. L'objectif de cette recherche était de déterminer quelles technologies pourrait améliorer les techniques courantes pour la détection de feux de forêts. L'observation par télédétection nous permet d'accumuler des données plus détaillées et précises que ceux provenant d'autres méthodes. Une analyse a alors été accomplie afin de comparer la précision des données thermiques et spatiales,

ainsi que la validité des données a différents intervalles de distances, la résolution et le cout de trois différents télédétecteurs infrarouge. Nos résultats démontrent que l'addition de technologies infrarouges dans les protocoles de détection en Ontario serait d'avantage et que des limits existent pour chacun des télédétecteurs testés dépendent sur l'altitude. Nos résultats indiquent que le FLIR Duo Pro R serait le télédétecteur le plus abordable dans les protocoles en Ontario selon les techniques examiner.

Introduction :

Forest fires are increasing in quantity globally on a yearly basis as fire activity is linked to weather and climate change (McFayden *et al*, 2020; Flannigan *et al*, 2009). Studies suggest that in the next century, because of global climate change, an increase of 50% in fire occurrence is to be expected (Harvey, 2016; Flannigan *et al*, 2009). Furthermore, a doubling of area burned is also to be expected due to anthropogenic activities (Harvey, 2016; Flannigan *et al*, 2009). This trend is obvious in Ontario, Canada where during the 2018 fire season the government observed nearly double the yearly average number of forest fires (MNRF, 2018). In the 2018 fire season alone, 1325 fires were observed in Ontario. This increase in forest fires is notable when compared to the 2017 fire season which recorded 749 fires and with the prior decade's yearly average of 750 fires (MNRF, 2018). We also observe similar increases in quantity, severity and size of forest fires in other countries such as the United States (McClure & Jaffe, 2018). This is especially true in the Northwest U.S. where there has been an obvious prolonging in wildland fire season linked to forest management techniques, as well as increased temperatures, earlier melting of snow, and increased dryness (Westerling *et al*, 2006).

Wildland fires occur as a result of dry weather, available fuel and ignition sources. Two main sources of ignition exist, the first being lightning and the second being human activities. Out of the 1325 fires observed in Ontario in 2018, approximately 29% of the fires were caused by anthropogenic activities and approximately 71% of the fires were due to lightning (MNRF, 2018). Wildland fire spread rates are influenced by temperature, relative humidity, precipitation and wind speeds.

As a result of global temperatures increasing by approximately 0.2°C per decade, many global changes have been observed (Hansen *et al*, 2010). These changes in the environment influence other parts of various ecosystems in a cyclical fashion. The temperature increase for

example, may have influenced global water cycles in an accelerated fashion thereby intensifying rainfall events, creating more prominent droughts and even modifying regional humidity trends (Dai, 2013; Dessler *et al*, 2008; Trenberth *et al*, 2003). In turn, regional water availability which is closely associated to regional droughts, can explain variations in burned area (Girardin *et al*, 2009). Changes in the climate are associated with global fire variations and are predicted to increase fire season severity over time (Flannigan *et al*, 2013).

Hotspot detection, the detection of areas of unusual outcome, meaning areas representing a cluster of heat signatures in forest fire detection, is an important part of forest fire prevention, monitoring and maintenance as it allows initial data on location and fire size (McFayden *et al*, 2020). The goal is to prevent injury and death to humans as well as to reduce secondary health hazards such as disease or illness related to smoke inhalation (from indirect contact). Protecting and monitoring environmental effects and reducing economic losses are also priorities (McFayden *et al*, 2020; MNRF, 2017).

Hotspot detection is not currently in use in Ontario protocols for forest fire detection. In order to understand current methodology in Ontario, it is important to review the history of fire detection in Ontario. This begins with the implementation of an organized forest fire protection division which has existed within the Ministry of Natural Resources and Forestry (MNRF) since 1885 (AFFES, 2019). In 1924, a new branch of the MNRF called the Aviation, Forest Fire and Emergency Services (AFFES) program was developed. This branch of the MNRF is responsible for responding to all natural disasters and for allocating resources to incidents. Through aviation, Ontario is able to get more detailed information on the location and size of fires. This allows decision makers to be better equipped when allocating fire resources (AFFES, 2019).

Ontario is divided into two regions. The Northwest Region includes Fort Frances, Kenora, Dryden, Thunder Bay, Nipigon, Red Lake and Sioux Lookout. The Northeast Region includes the Haliburton, Sudbury, Timmins, Chapleau, Wawa and Cochrane sectors (AFFES, 2019). All sectors are monitored using aerial detection. The goal of the aerial detection program is to detect fires when they are small in order to have a better chance at controlling them (AFFES, 2019).

The actual procedure involved in aerial detection in Ontario, uses pilots and observers who are trained through an MNR course called AV109 (AFFES, 2019). Observers are assigned a detection flight path and are flown by detection pilots in one of ten aircraft (Cessna Skymaster 337). Observers follow an observation protocol involving looking out of the window of the aircraft for visible smoke. This is currently the most reliable signal for daytime visual detection of forest fires (McFayden *et al*, 2020; Zimmerman, 1969; Byram & Jemison, 1948).

Although all observers and pilots hired for detection go through the same training, the information provided is relative to the perspective of the observer (AFFES, 2019). For example, if an observer is not paying attention a small fire could be missed. Furthermore, an inaccurate location or fire size could be reported as a result of an observer being inexperienced. Human vision is limited by several factors such as acuity, sensitivity to light, attention of the observer; the size, distance and intensity of the target and visibility factors such as haze, fog and dust clouds (Byram & Jemison, 1984). An increase in interest for automatic surveillance and early fire detection has started to take precedence over traditional human surveillance as a result of this subjectivity and the effects it has on detection reliability (McFayden *et al*, 2020; Arrue *et al*, 2000). Detection reliability is the biggest problem recognized in the context of the creation of forest fire detection systems.

While aerial surveillance by use of observers has been used to identify burning areas, remote sensing offers similar methods of detection without relying on human vision or smoke for the detection of fires. Remote sensing is defined as the acquisition of information of an area without making physical contact with it (Robert, 2007). In the case of infrared sensors for forest fire detection this means flying sensors over areas of forest using airplanes, helicopters, drones or satellites in order to gain information on these areas. This works by using sensors which convert the energy information accumulated to receiving and processing software which create images with the data. The image data is then used to interpret findings (Joseph, 2011).

Infrared is defined as electromagnetic radiation with wavelengths longer than the visible light spectrum (Liew, 2017). These wavelengths, which are invisible to the human eye extend from 700 to 1,000,000 nanometers and are located near the red edge of the visible spectrum from which they received the name infrared (Liew, 2017). These wavelengths have frequencies which range from 300 GHz to 430 THz (Haynes, 2011).

The heat emitted by fires is a detectible signal for sensors that are able to detect the thermal infrared portion of the electromagnetic spectrum. Heat is transported by the fire in several different ways – convection, conduction, and radiation. The radiated heat is the main signal that these sensors are able to detect (Allison *et al*, 2016). This follows Planck's law, which describes spectral radiance distribution as a function of wavelength on the emitted electromagnetic radiation scale (Kuenzer & Dech, 2013). This allows the detection of emitted thermal radiation by targets and in the world of forest fires can allow early detection of fires. (Arrue *et al*, 2000).

The use of remote sensing technologies in forest fire detection is not standardized across Canada as forest fire detection protocols vary from province to province. Infrared sensing has

been explored as a means of false alarm reduction in some studies (Arrue *et al*, 2000; Ollero *et al*, 1999; Ollero *et al*, 1997). These studies have demonstrated the usefulness of IR technologies in the assistance of other technologies such as red-green-blue (RGB) imagers (Arrue *et al*, 2000). Most imaging techniques concentrate on the mid-wave infrared (MWIR, 3-5 μm) or thermal infrared (TIR, 8-15 μm) regions (Dozier, 1981). TIR sensors have the advantage of being able to see through smoke cover because even thick smoke is transparent at these wavelengths. The dynamic range of the scene in TIR is also limited making it easier to get high contrast imagery of both the heat source and the background (Allison *et al*, 2016).

Different airborne sensor platforms exist for monitoring (Allison *et al*, 2016). This paper concentrates on airborne sensing using fixed-wing aircraft and Unmanned Aerial Vehicles (UAV) specifically. This is because these platforms allow for more maneuverability, can be more easily deployed, can target priority areas and can revisit often and for longer periods than other available platforms. Watch towers for example, are inflexible, need to be carefully placed, are expensive, and are not suited for large, sparsely populated areas (McFayden *et al*, 2020; Allison *et al*, 2016). The use of UAVs has also come into the light recently as a possible addition to current fire practices. UAVs provide rapid maneuverability, personnel safety, and allow faster data acquisition than relying on satellite data (Yuan *et al*, 2015). However, UAVs depend on internal batteries which limit range. The stability of the aircraft over the fire is also an issue for small UAVs (Hinkley & Zajkowski, 2011). Also, the ability of UAVs to collect imagery requires them to be flying directly on top of the area being studied and due to fire severity and the height of the vegetation being burned, limitations exist (Ollero, 2006).

The time of day at which sensors are being flown, is another consideration in the planning of aerial detection (McFayden *et al*, 2020; Allison *et al*, 2016). Daylight airborne

remote sensing allows for smoke detection and light level allow for increased safety during flights and easier target detection (Allison *et al*, 2016). However, daylight detection has its own set of disadvantages as it is susceptible to the effects of reflected sunlight for MWIR sensing. These effects include false positives due to solar heated rocks and other objects (Allison *et al*, 2016). Forest fires are known to be diurnally cyclical in terms of size and intensity. These characteristics are known to be decreased markedly overnight (Wooster *et al*, 2013). Therefore, although nighttime sensing (which is focused on bright object detection) allows a higher contrast between hotspots and background temperatures, and negates effects of reflected sunlight, it may not provide a completely representative image of active fires (Allison *et al*, 2016). Therefore, flights need to be timed properly depending on the sensor being used. Current detection flights in Ontario, take place during daylight hours and as such the infrared remote sensors being added to current practices would need to be able to function properly during daylight in order to be viable additions.

Since the current methods used for the detection and monitoring of forest fires operate with such variability in success rates and since increasing fire occurrence could affect the functionality of these methods, this study proposes the use of various remote sensing systems as alternate or additional methods of hotspot detection for fire prevention and monitoring. The goal is to develop methods for more efficient identification of potential fires using remote sensing to provide support to current fire detection practices.

The present work deals with the application of infrared sensing technologies used for hotspot detection and fire management activities from aircraft in early fire detection. Rapid, accurate, and objective methods to quantify fire fuels are needed to evaluate the effectiveness of current fire practices as well as to improve upon them. Therefore, the spatial accuracy, thermal

accuracy, and ability to determine accurate sizes of hotspots were examined for several remote sensing technologies. The focus of this study was to determine which of the infrared remote sensors tested could be a useful addition to current methodology. We focused on off-the-shelf infrared remote sensors and wanted to find the least expensive option that would be beneficial to current practices. The intent is to provide information that could be used to develop a new protocol for Ontario and for widespread deployment in wildland fire management in order to allow for greater resource management and allocation, as well as to reduce health effects related to forest fires.

Materials and Methods:

Study site:

The study area was located 1.2 NM (2200 m) southeast of Alban, Ontario, Canada at the French River/Alban Aerodrome (DMS: 46° 5' 36" N, 80° 36' 15" W). This is a private airport with two turf runways. The first runway (Runway 1) runs North/South and has a length of 750 m. The second runway (Runway 2) runs East/West and is 760 m in length (See Figure 1) (Nav Canada, 2019). Butane heaters were used to mimic fire hotspots and were set up on runway 2.



Figure 1. Demonstrates the location of the study site (Google Earth, 2020). The inset image demonstrates a satellite image of French River/Alban aerodrome this represents an aerial view of the area being flown over during experimentation (Google Maps, 2019). Runway 1 runs parallel to highway 607. Runway 2 runs approximately at a 90° angle to Runway 1.

Sensors:




Three sensors were used for this research (see Table 1). All sensors were nadir mounted, that is, looking straight down from the aircraft.

The first sensor used in this study was the ITRES microTABI (μ TABI), which is a broadband, wide array, cryo-cooled pushframe thermal imager. This sensor has a reported spatial resolution of 0.7 m with a flight line swath of 1200 m at an aircraft speed of 56.58 meters per second (110 knots) and an altitude of 1730 m AGL. This sensor is considered to be a mid-wave infrared (MWIR) sensor as it has a spectral range of 3.7 - 4.8 μm (Table 1).

The second sensor, the FLIR Duo Pro R (Pro) is an HD dual-sensor thermal camera. It is a combined high resolution radiometric thermal imager and 4K color camera. This sensor has an uncooled VOx Microbolometer. This sensor is considered a thermal infrared (TIR) sensor as it has a spectral range of $7.5 - 13.5 \mu\text{m}$ (Table 1). The pixel resolution for the thermal portion of this sensor is of 336×256 with pixels of $1.85 \mu\text{m}$ in size.

Lastly, the FLIR Duo (Duo) was the third sensor used throughout this research. This is an uncooled radiometric thermal and visible light imager that was designed for professional drone applications. This sensor has been discontinued as of November 1st 2018. This sensor is considered a thermal infrared (TIR) sensor as it has a spectral range of $7.5 - 13.5 \mu\text{m}$ (Table 1). The pixel resolution for the thermal portion of this sensor is of 160×120 with pixels of $12 \mu\text{m}$ in size.

Table 1. List of sensors and their specifications

	microTABI- 640	FLIR Duo® Pro R	Duo R
Sensors			
Price	Approx \$100,000	Approx \$6,000	Approx \$3,000
Dimensions (mm)	100 × 230 × 250	85 × 81.3 × 68.5	41 × 59 × 29.6
Weight (g)	3800	325	84
Spectral range (μm)	3.7-4.8	7.5-13.5	7.5-13.5
Spectral Channel	1	1	1
Max Frame rate (Hz)	90-110	30	8.3
Operating Temperature (°C)	0 to 40	-20 to 50	0 to 50
Thermal Measurement accuracy	Not Available	±5°C or 5% of readings in the -25 to +135°C range ±20°C or 20% of readings in the -40 to +550°C range	± 5 °C or 5% of reading
Field of View (°)	40	25-45 (depending on lens)	57x44 (90 on visible camera)
Maximum Altitude	10000ft/4500m	38000ft/11582m	12000ft/3657m
Sensor Resolution	640x512	4000x3000 (thermal 640x512)	1920x1080 (thermal 160x120)
GPS	GNSS or MEMS (external)	GLONASS	none
Output Format	BIP (ENVI compatible)	Analog/Digital video (1080p mov/tiff/rjpg)	Analog/Digital video (1080p mov/tiff/rjpg)

Aircraft:

Three different aerial platforms were used during this study. These include the Aero Commander 500. This is a six-seat, high wing, fixed-wing, twin piston-engine aircraft. Standard configuration allows for mission equipment and two pilots. This aircraft was used to acquire μ TABI data and was flown at 640.8 to 2590.8 m Above Ground Level (AGL) at an average speed of 90 metres per second (175 knts). The μ TABI was internally mounted in the Aero Commander 500.

The Cessna 172 Skyhawk which is a four-seat, single engine, high wing, fixed-wing aircraft made by the Cessna Aircraft Company was also used in data acquisition. The Cessna 172 was used to fly the FLIR Pro and FLIR Duo sensors at altitudes of 304.8 and 609.6 m AGL. A SkyIMD camera mount was used for this data collection. This is a strut mount that is customizable for use with smaller sensors. This aircraft flew at 51.44 meters per second (100 knts) for each pass.

A DJI Matrice 600 was used in this study. This is an Unmanned Aerial Vehicle (UAV), specifically a drone. The aircraft was remotely piloted from the runway and the sensors were placed one at a time on a gimbal mount and flown at 60.96 and 121.92 m. The sensors used on this aircraft were the FLIR Pro and the FLIR Duo. This UAV was set to fly at 8.93 metres per second (17.37 knts) for each pass.

Flight plans:

Several altitudes were flown in order to compare the effects on spatial resolution as well as spatial and thermal accuracy. The planned altitudes for flights were between 60.96 and 2590.8 m AGL. These altitudes were modified according to conditions and to the restrictions of the sensor and aircraft being used.

In the case of the *u*TABI, in order to have the most accurate data, flight lines were flown at several altitudes in the same direction each time. This was done in order to account for positional bias seen in previous data collection trials. The line at each altitude was flown down the center of the polygon.

*u*TABI data collection was done on June 21st 2019 in Alban Ontario. Conditions were ideal for IR scanning; this means the flights took place in low wind < 10 km/h with clear skies. The weather report for that day indicates that the temperature was at a low of 22°C and high of 23°C with passing clouds and an average humidity of 53%. At the time of each pass there were no clouds overhead.

Both the FLIR Pro and FLIR Duo were flown on the 15th of August 2019 in Alban Ontario. Conditions were ideal for IR scanning, the weather report for that day indicates that the temperature was at a low of 13°C and high of 23°C with broken clouds and an average humidity of 58%.

*u*TABI:

The *u*TABI was flown on the Aero Commander 500 over the five heaters on June 21st 2019. The aircraft was over the targeted area by 5:20 am. The altitudes flown were of 883.92, 1097.28, 1310.64, 1524, and 1767.84 m AGL

Pro and Duo:

These sensors were flown individually on a Cessna 172 on August 15th 2019. These sensors were attached to the aircraft on an external wing strut mount. The flight took off at 11 am from the French River/ Alban aerodrome. The altitudes flown were 307.54 and 609.6 m AGL. These sensors were also flown at 60.96 and 121.92 m AGL using a UAV.

Hotspots:

uTABI:

Five butane heaters were set up on the runway at the French River/Alban aerodrome. The space between heaters 1 and 2 was 13 m. The space between heaters 2 and 3 was 15 m. The space between heaters 4 and 5 was 22 m. Heaters 3 and 4 were set up at a shorter distance of 4 meters in order to identify at what altitude these two heaters were represented by a single point. Heaters 1, 4, and 5 were all set to the same heat setting and had an average temperature of 335°C. Heater 2 was set to the lowest temperature setting with an average temperature of 244°C. Finally, Heater 3 was set to the highest temperature setting with an average temperature of 430°C. See Figure 2 for representation of heater set up. The GPS coordinates for each heater were also recorded (Table 2).



Figure 2. Demonstrates heater placement and temperature plan. A represents the heater set up on June 21st, 2019 this is the set up for the uTABI data the heaters are represented by blue points on runway 2. B represents the heater set up on August 15th 2019, this is the set up for the Duo Pro R and Duo R the heaters are represented by pink points on runway 2. Each point on the image represents a heater. Heaters 1 to 5 are displayed from right to left.

Table 2. List of heaters and their coordinates

	Coordinates	
	Latitude	Longitude
Heater 1	46.09122015	-80.60574673
Heater 2	46.09122327	-80.60581648
Heater 3	46.09121599	-80.60589059
Heater 4	46.09120465	-80.60597589
Heater 5	46.09120834	-80.60599226

Pro and Duo:

Five butane heaters were set up on the runway at the French River/Alban aerodrome. Heaters 1, 2, and 3 were set up at approximately 5.5 meters apart. The space between heaters 1 and 2 was 5.41 m. The space between heaters 2 and 3 was 5.79 m. The space between heaters 3 and 4 was 6.72 m. Heaters 4 and 5 were set up at a shorter distance of 1.33 meters in order to identify at what altitude these two heaters were represented by a single point. Heaters 1, 4, and 5 were all set to the same heat setting and had an average temperature of 382°C. Heater 2 was set to the coolest temperature setting with an average temperature of 245°C. Finally, Heater 3 was set to the highest temperature setting with an average temperature of 428°C. See Figure 2 **B** for representation of heater set up. The coordinates for each heater were also recorded (Table 2).

Temperature readings from the ground:

Temperature readings of each heater were taken from the ground using laser thermometers. The Extech Instruments Dual Laser IR Thermometer with Color Alert was used for each hotspot. Readings were taken and recorded three times for each heater, one reading was taken before the flight, one during and one right as the planned flight lines were finished before turning the heaters off. These temperature readings were taken from the center of each heater at a distance of approximately 12 inches. The readings were taken from the center of the heaters to ensure a representative reading. A ground temperature reading near the area of the heaters was also taken

as a reference for background temperature the average reading on June 21st was 9°C. The average reading for background temperature on August 15th was 29°C.

Resolution:

The ability to differentiate between each individual heater was recorded for each altitude.

Ground sampling distance (GSD) which is the distance from pixel center to pixel center, was calculated for the *u*TABI at each altitude.

Spatial Accuracy:

Coordinates of butane heaters were recorded from the ground using a Garmin eTrex 10 handheld global positioning system (GPS). The distance between projected aerial coordinates and ground coordinates was measured in meters in order to determine the range of accuracy for the ITRES *u*TABI data. This measurement was not able to be completed with the data from the FLIR Pro or the FLIR Duo. The diameter of each heater was also taken from the aerial data at each altitude from the *u*TABI data. This data was collected by measuring the diameter of the heat signature for each heater at each altitude.

Thermal accuracy:

The hottest pixel from each heater was selected for each altitude flown from the *u*TABI data.

The number of hot pixels for each heater was also obtained for all of the infrared data used (*u*TABI, Pro, Duo).

Results:

uTABI:

Resolution:

A Pearson correlation was done to determine if an association exists between altitude and spectral resolution (GSD). This showed a significant positive association between altitude and GSD [$r(5)=1$, $p<.001$].

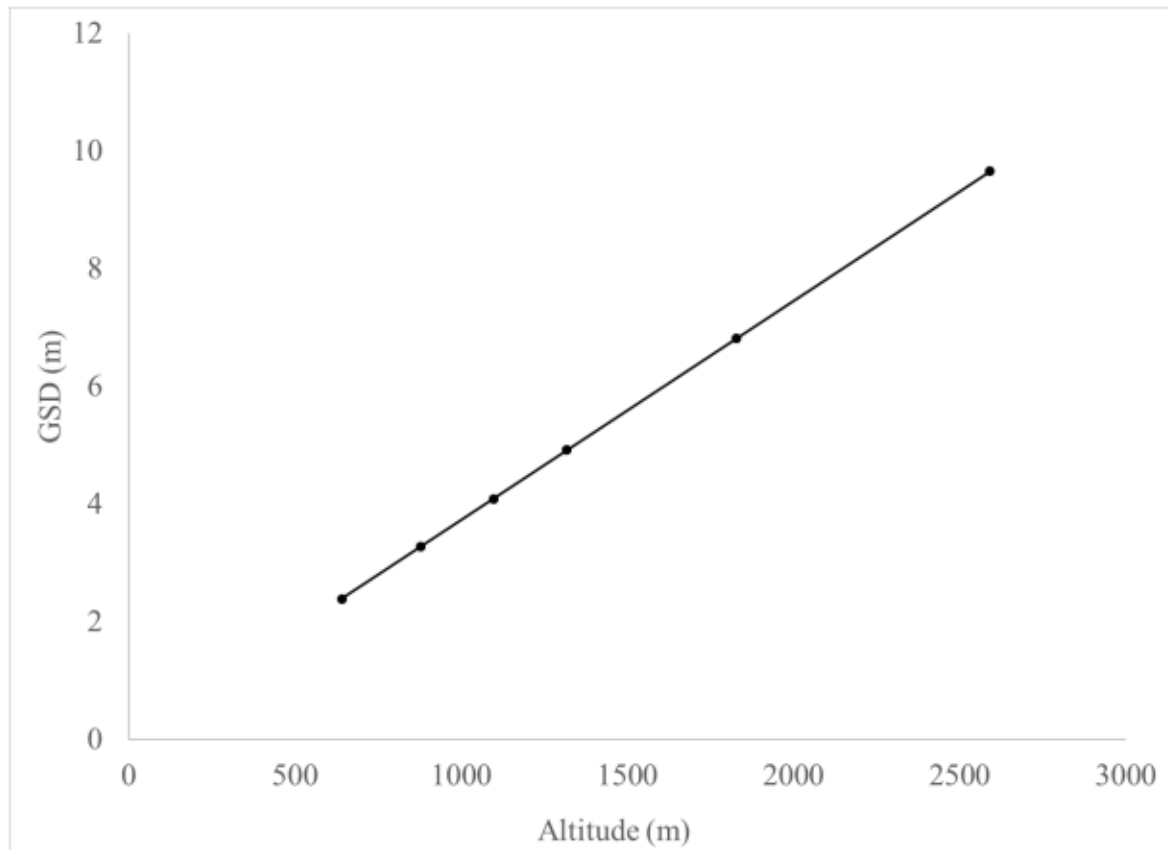


Figure 3. Demonstrates the relationship between ground sampling distance (GSD) in meters and altitude in meters for ITRES uTABl. [$r(5)=1$, $p<.001$, $R^2 = 1$]. A single independent observation was used to derive these values at each altitude.

Spatial accuracy:

A Pearson correlation was done to determine if an association exists between altitude and average spatial variance. This showed a significant positive association between altitude and average spatial variance [$r(5)=.98$, $p<.001$]. See Figure 4.

A Pearson correlation was also done to determine if an association exists between altitude and diameter of heat plumes (Figure 5). This showed a significant positive association between these variables, [$r(5)=.98$, $p<.001$].

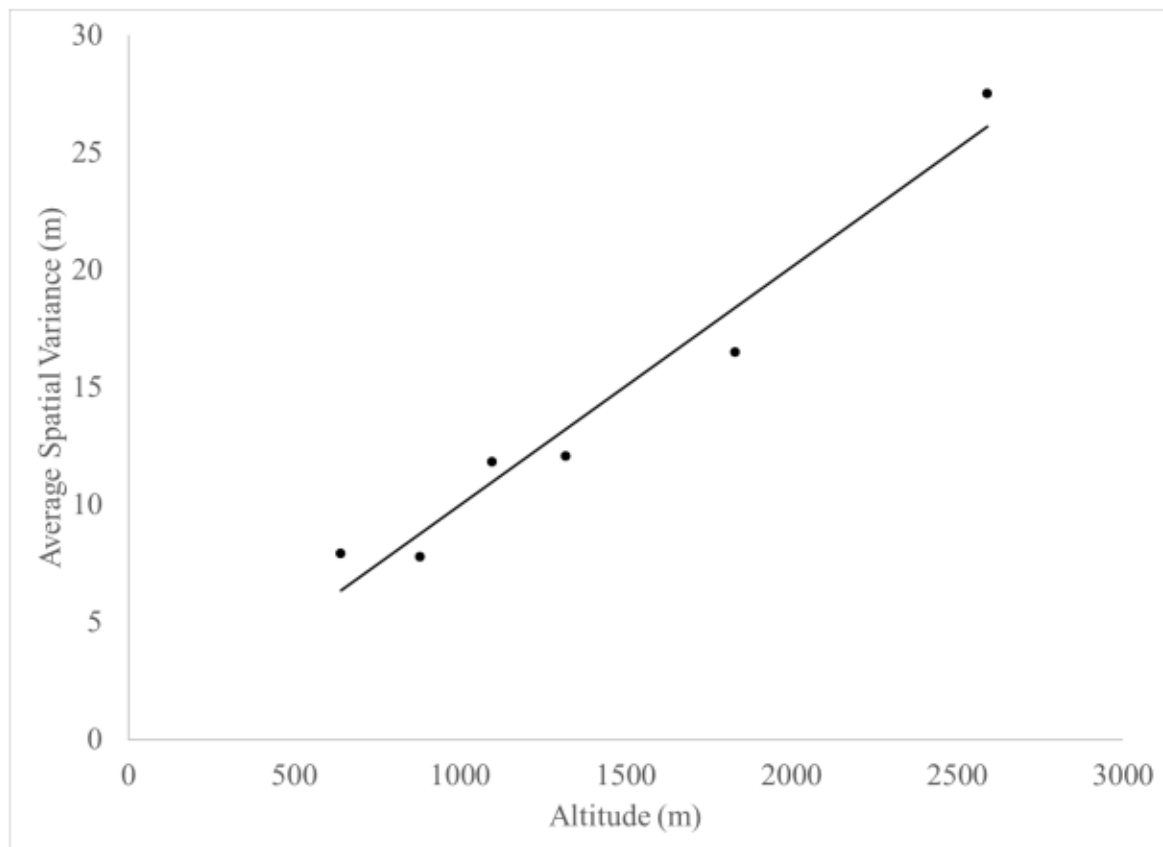


Figure 4. Demonstrates the relationship between average spatial variance in meters and altitude in meters for ITRES uTABI data. [$r(5)=.98$, $p<.001$, $R^2 = 0.9596$]. *A single independent observation was used to derive these values at each altitude.*

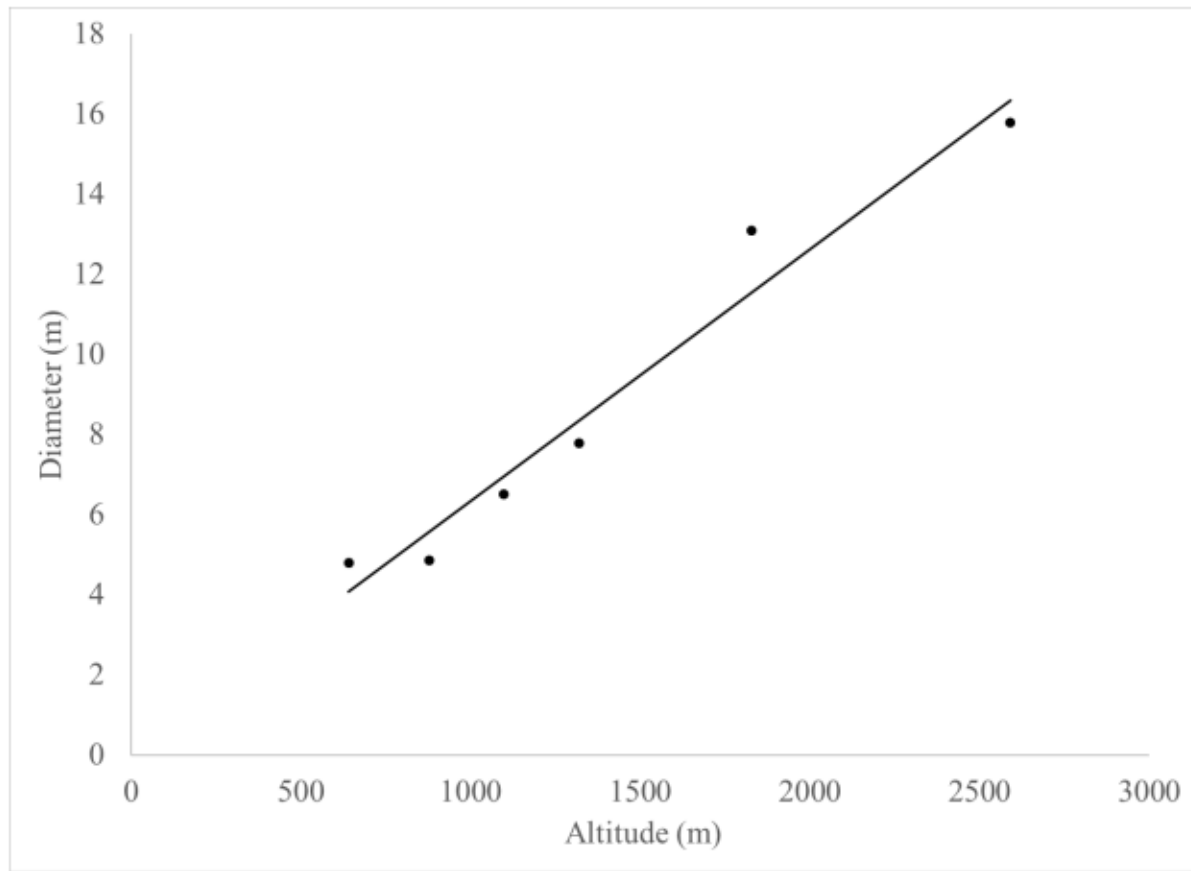


Figure 5. Demonstrates the relationship between diameter in meters and altitude in meters for ITRES uTABI data. [$r(5)=.98$, $p<.001$, $R^2 = 0.9595$]. A single independent observation was used to derive these values at each altitude.

Thermal accuracy:

A Pearson correlation was done to determine if an association exists between altitude and the ability to detect the hottest pixel. This showed a significant negative association between these variables, [$r(5)=-0.95$, $p=.002$]. This data also demonstrates that on average Heater 3 represents the highest pixel temperature and that Heater 2 represents the lowest pixel temperature.

A Pearson correlation was done to determine if an association exists between altitude and the number of measured pixels (hot). There was no significant correlation, [$r(5)=-0.55$, $p=.259$]. As altitude increased the amount of pixels did not seem to decrease. The average number of heated pixels for each heater at each altitude demonstrates that Heater 3 consistently represents the

largest quantity of pixels (92.75) and that the Heater 2 consistently represents the lowest count of heated pixels (32).

Pro and Duo:

Resolution:

The GSD for the *u*TABI increased with altitude, meaning that the size of each pixel increases with altitude (Figure 3). This indicates that with increasing altitude resolution decreases. When plotted, 100% of change in resolution (GSD) are accounted for by a change in altitude. The results (Figure 6) demonstrate that the FLIR Pro is capable of detecting each individual heater from 60.96 to 609.6 m AGL. The FLIR Duo (Figure 7) is capable of detecting each individual heater from 60.96 to 121.92 m AGL only. The imagery demonstrates that at altitudes of 304.8 and 609.6 m AGL the infrared imagery is unable to detect heat sources the size of our heaters. The Duo at 640.8 m AGL is however still able to detect the heaters in its 4K colour imagery. At 609.6 m AGL however, even the 4K colour portion of the sensor is out of range for heaters of that size.

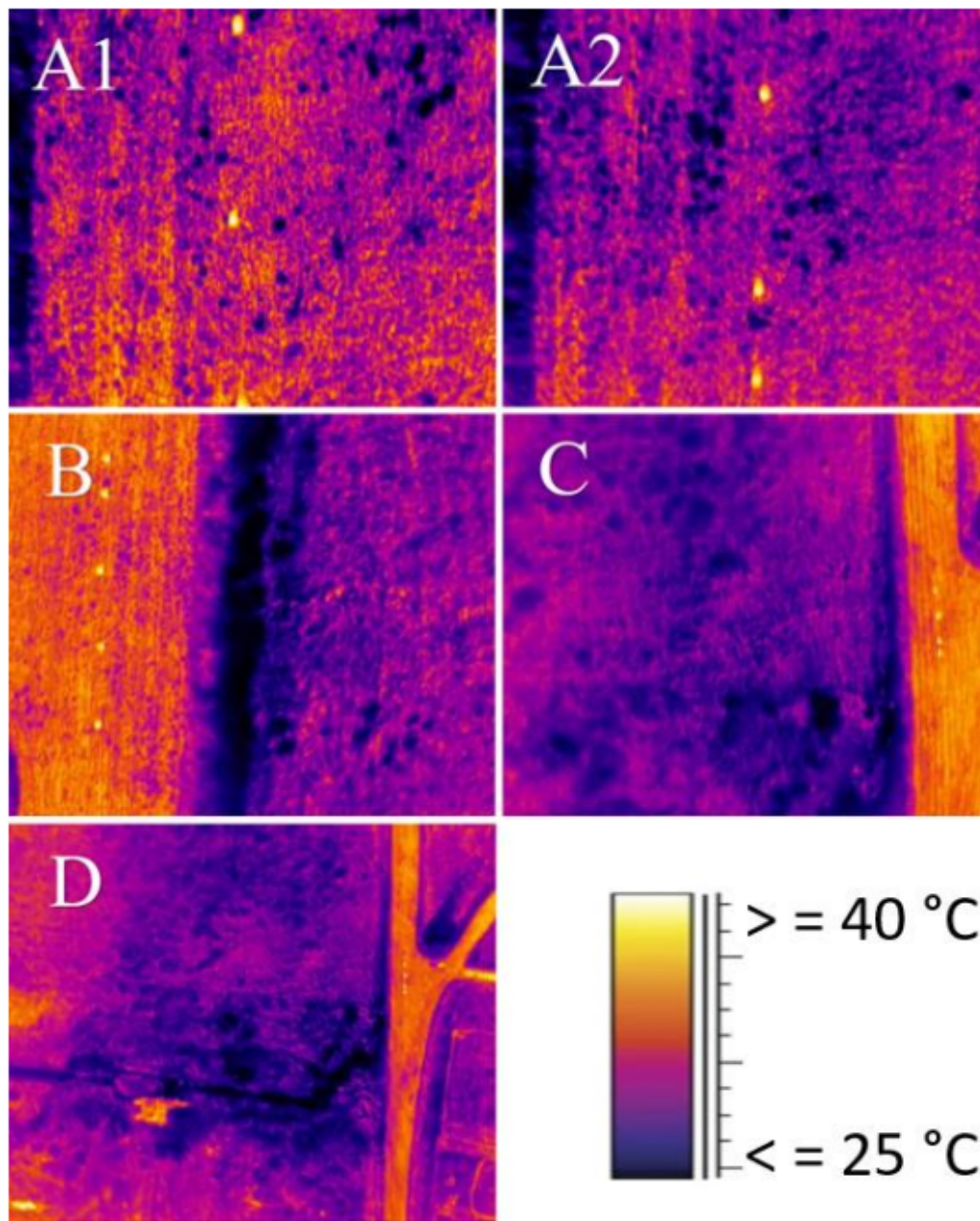


Figure 6. Demonstrates the aerial infrared view of hotspots from FLIR Duo Pro R. A1 represents heaters 1 and 2 from top to bottom at 200 ft AGL. A2 represents heaters 3, 4 and 5 from top to bottom at 200 ft AGL. B represents heaters 1 to 5 from bottom to top at 400 ft AGL. C represents heaters 2 to 5 from top to bottom at 1000 ft AGL. D represents heaters 2 to 5 from top to bottom at 2000 ft AGL. Yellow points in the center of the runway indicate the butane heaters.

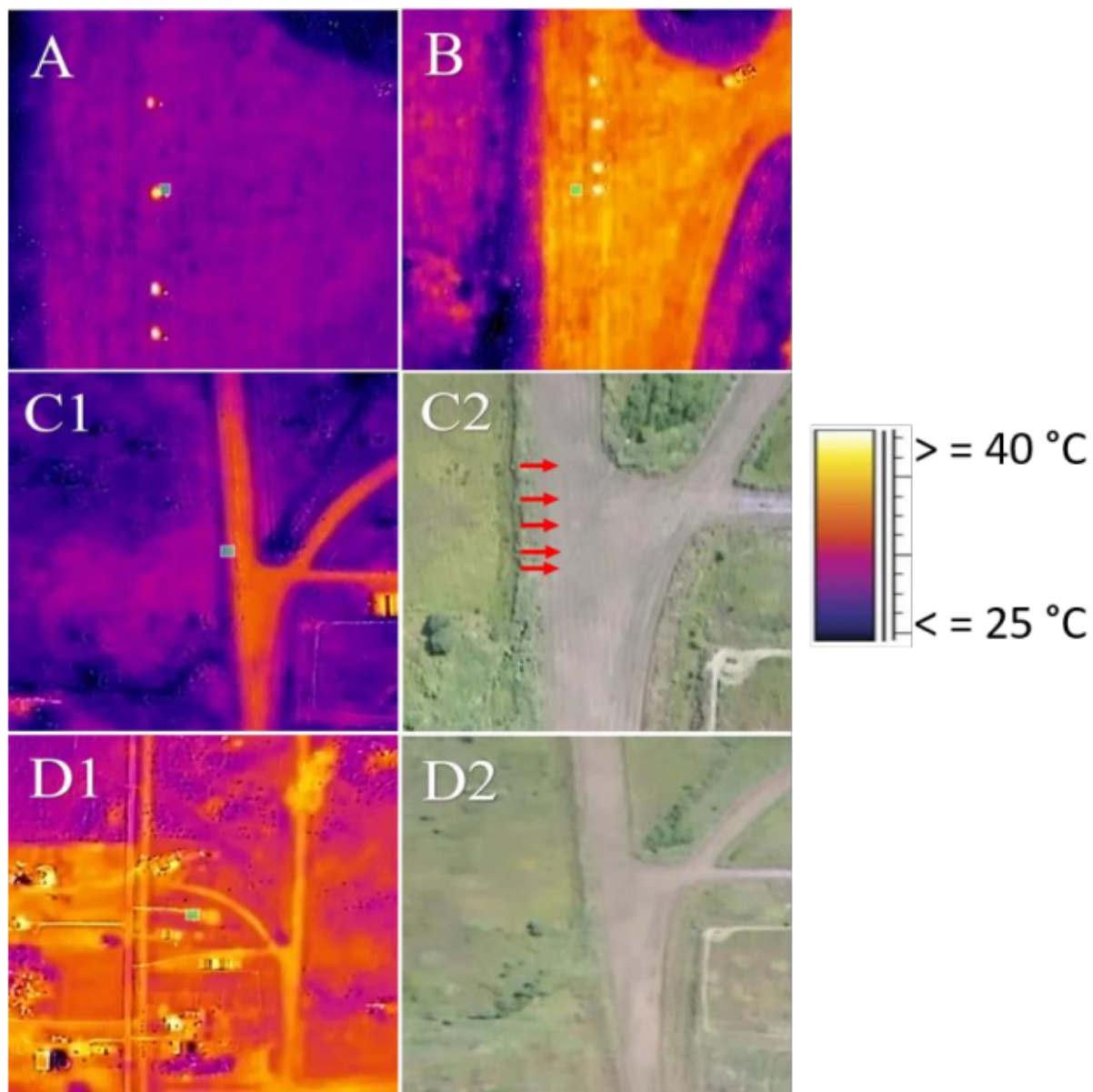


Figure 7. Demonstrates the aerial infrared view of hotspots from FLIR DUO R. All photos represent heaters 1 to 5 from top to bottom. Heater 1 is out in all of the images of this set. **A** represents the infrared view from 200 ft AGL. **B** represents the infrared view from 400 ft AGL. **C1** represents the infrared view from 1000 ft AGL. **C2** represents the RGB view from 1000 ft AGL, the arrows demonstrate the placement of the heaters. **D1** represents the infrared view from 2000 ft AGL. **D2** represents the RGB view from 2000 ft AGL. Yellow points in the center of the runway indicate the butane heaters.

Thermal accuracy:

FLIR Pro and Duo data was combined in order to account for the small sample size for the Duo.

A Pearson correlation was done to determine if an association exists between altitude and the

number of measured pixels (hot). There was a negative significant correlation, [$r(5)=-0.856$, $p=.029$]. As altitude increased the amount of pixels did seem to decrease. The average number of heated pixels for each heater at each altitude demonstrates that Heater 3 consistently represents the largest quantity of pixels (227) and that the Heater 2 consistently represents the lowest count of heated pixels (98).

Table 3. Number of high temperature pixels associated to each heater per trial.

Sensor	Altitude (ft. AGL)	Heater 1	Heater 2	Heater 3	Heater 4	Heater 5
FLIR	2000	N/A	18	31	26	23
Duo	1000	N/A	49	84	59	52
Pro	400	106	87	132	114	103
R	200	275	176	275	184	238
FLIR	400	N/A	80	175	141	127
Duo	200	N/A	116	279	179	198
R						

Discussion:

Data collection is complicated for the evaluation of sensor technologies for wildland fire detection as sensor performance and capabilities are usually tested in laboratory measurements as opposed to in the field (Allison *et al*, 2016). Therefore, the majority of prior research has been done through demonstrated projects as opposed to controlled studies (Ambrosia *et al*, 2011; Kontoes *et al*, 2009; Merino *et al*, 2006). This is due to the unpredictability and complexity of fires (Allison *et al*, 2016). Studies involving wildland fire detection commonly involve measuring detection distances or rates for staged events such as controlled burns or field trials in actual use (Allison *et al*, 2016). The variety of data available for our use is thus limited. However, this is a pilot project and the trends discovered throughout this project are essential for the development of modifications for larger scale application.

Resolution:

The results for GSD for the *u*TABI demonstrate that as altitude increases GSD increases.

Resolution is best when GSD is small therefore, as altitude increases resolution decreases. This was the expected result for all sensors as it is commonly the case that with increasing altitudes data resolution decreases quite rapidly (Penížek *et al*, 2016). The visual data from both the FLIR Pro and Duo demonstrate similar results, as altitude increases the ability to see the heaters decreases and as a result accuracy decreases.

This was the expected result as the inverse square law states that a specified physical quantity is inversely proportional to the square of the distance from the source of that physical quantity (Adelberger *et al*, 2003). This means that at a certain height, which in this case is 1006 m, the accuracy begins to diminish greatly (see spatial accuracy).

In terms of the application of infrared technologies for forest fire detection protocols this means that the altitude being flown needs to be taken into consideration depending on the sensor being used in order to optimize spectral resolution. This is important for forest fire detection because it allows us to determine a range for which each sensor performs within specific spectral resolution criteria. This allows us to determine guidelines for altitude in order to maintain consistency in spectral resolution no matter what sensor is being used. Basically, it allows us to develop guidelines for the maximum altitudes each sensor can be flown at in order to accurately detect fires. Accuracy will always be improved with lower altitudes where appropriate.

Spatial accuracy:

The average spatial variance values, which are the measurements of distance between the coordinates on the ground to the proposed coordinates from the aerial data increase with increasing altitudes. When plotted (Figure 4) 95.96% of change in accuracy is accounted for by a change in altitude. Therefore, as altitude increases accuracy in meters decreases as the difference

between ground and aerial data becomes larger. Once again, this data was from the *u*TABI as the FLIR sensors were not capable of detecting this information.

If we base our protocol on that of the Hinton Grid Test in Alberta, which is the standard for Canada, spatial accuracy needs to fall within a quantifiable distance of 10 m. In looking at the results there is a clear demarcation where our data falls within that range, at any altitude under 1006 m spatial accuracy is within 10 m. Our protocol for flying in Ontario would then include this guideline of 1006 m AGL being the maximum altitude for the application of infrared remote sensing using the *u*TABI.

The average diameter of heaters increases in the aerial data with altitude. When plotted 95.95% of change in diameter is accounted for by a change in altitude. Meaning that, the data suggests that the thermal plumes for each heater are becoming larger the higher the sensor is flown, when in reality they are stable in terms of size. Because this is being measured from infrared data, we are measuring the diameter of the plume and not of the heater itself. This result indicates that the ability to determine the diameter of a fire accurately from the air decreases with increasing altitude. Again, due to the inverse-square law. However, it is still possible to differentiate between the hottest and coldest heaters (3 and 2 respectively) at every altitude. This means that it would be possible to determine when a thermal plume is larger in relation to another but not to determine the exact diameter of a fire from infrared remote sensing technologies such as the ones we have tested. Based on our results hotter heat sources project more high temperature pixels and thus a larger diameter could indicate either a larger fire or a hotter one. It would however be difficult to determine whether the readings are displaying a larger fire or a hotter one. Nevertheless, both are factors that indicate fire behaviour and could be useful for detection and monitoring of forest fires.

Thermal accuracy:

The average heat for the hottest pixel for each heater at each altitude demonstrates that as altitude increases thermal accuracy, the ability to determine a temperature on the ground from aerial data, decreases. This data was acquired only with the μ TABI as the FLIR sensors were not of high enough quality to be able to detect heat signatures for each pixel within an image. The aerial results demonstrate temperatures from 7°C to 40°C which is not an accurate representation of the temperatures as the recorded temperatures from the ground range from 230°C to 442°C. This is explained by the fact that the heat plumes bleed out and are averaged out by surrounding unheated pixels. This leads to the heat sources being detected at much lower temperatures from the air and as altitude increases these temperatures decrease even further. However, it is still possible to detect the heaters as the difference between them and ground temperatures is great enough. It is also possible to differentiate between the hottest and coldest heaters (3 and 2 respectively) at every altitude. This means that it would be possible to detect fires and determine if a fire is hotter than another in relation to each other but not to determine the exact temperature of a fire from infrared remote sensing technologies such as the ones we have tested.

Although the data for the μ TABI sensor demonstrated no significant correlation between altitude and the decrease in quantity of hot pixels, the data for both the Pro and Duo did demonstrate significant correlations. This indicates that as altitude increases the number of represented hot pixels decreases. This is because the resolution results indicate that the size of the pixels increases with altitude and as such, fewer are used to represent an area of the same size (see inverse-square law). This was the expected result however, this data was still collected in order to provide some information on thermal accuracy for the Pro and Duo which were not able to give temperature readings for each pixel in the image data collected. The data also showed that for each sensor the average number of heated pixels for each heater at each altitude

demonstrates that Heater 3 consistently represents the largest quantity of pixels and that the Heater 2 consistently represents the lowest count of heated pixels. This was the expected result as Heater 3 represents the hottest heater and Heater 2 represents the coldest heater in all trials. This is a well-known result of increasing altitude but was done in order to demonstrate the same trends using our sensors and to be able to compare the function of our sensors to each other. We were able to see with these results that the differentiation of the hottest and coldest heaters was made possible and this is important information for the application of these sensors into current forest fire detection protocols in Ontario.

These findings suggest that concentrating on the number of hot pixels could be a good indicator of temperature as it is possible to differentiate between hotspots of different temperatures based on pixel count.

In low altitude imaging, saturation is an issue that is not easily avoided with less specific technology (Allison *et al*, 2016). The difference between the image of a fire that fills one pixel and its background is large and can exceed the dynamic range for the sensor. For detection, a saturated pixel can still be indicative of a fire (Allison *et al*, 2016; Matson & Dozier, 1981;). However, in radiometric measurements saturation needs to be avoided in order to get accurate readings. Thermal accuracy for both the FLIR Pro and FLIR Duo were analysed in relation to themselves as a result as the saturation of pixels was obvious. This means that pixels that were representative of our heat sources (heaters) made surrounding background pixels appear as high temperature spots. We can therefore conclude that all three sensors are able to differentiate targets of different temperatures when data is acquired within each sensors specific altitude ranges.

Limitations:

As this was a preliminary study to identify the validity of the implementation of the FLIR Duo Pro R, the FLIR Duo R and the ITRES *u*TABI into current methodology for forest fire detection in Ontario, several limitations exist. Atmospheric temperature and humidity were not corrected for these sensors, the impact of meteorological factors on testing have been shown to be considerable and should be corrected for in future research (Tran *et al*, 2017). These corrections could be useful in the identification of limitations for each of these infrared sensors. One study showed that active thermography is more apparent in high ambient temperature and humidity conditions and this information could be applied to any further staged testing. In forest fire detection work for Ontario these sensors would primarily be used to collect presence/absence data. This means that although several meteorological corrections were not done, our data still allowed us to determine some of the limitations of our sensors because we could still determine whether or not our sensors could detect heat sources (hotspots) the size of our butane heaters. Staged testing is primarily done over field trials for testing infrared remote sensing technologies and the use of meteorological corrections would be useful in those settings. As previously mentioned, this is a pilot project and the trends discovered throughout this project are essential for the development of modifications for larger scale application in Ontario forest fire detection protocols.

Furthermore, the influence of wind was not taken into consideration as a wind reading for the specific area being studied was not available, the general area of greater Sudbury showed wind speeds of less than 10 km/h however no corrections were made to the data to account for wind. Wind can affect temporal readings and should be taken into consideration in future research (Leblon *et al.*, 2012).

Lastly, the number of independent observations used to derive our findings was small due to the fact that we were using airplanes which were being used simultaneously for ongoing forest fire detection across Ontario. Therefore, availability of the aircrafts for experimentation purposes was limited. Furthermore, the costs associated with data collection of this sort were elevated which is why we wanted to establish preliminary findings with a pilot study before doing a study with an increased amount of passes over our heaters. In future, a reproduction equation should be used to calculate the basic reproduction number which should be used during experimentation in order to assure reproducibility and consistency.

Conclusion:

Our data suggests that as altitude increases resolution, accuracy in meters, ability to determine the diameter of a fire and ability to determine a temperature on the ground from aerial data decrease. This is due to the inverse-square law. Limitations exist for each of the sensors in different contexts. The FLIR Duo for example is useful for low altitude UAV applications but does not perform adequately at higher altitudes. This sensor could not be used on detection flights as a result as typical detection flights fly at around 640.8 m AGL. The hotspots are not identifiable in the imagery acquired by this sensor at 640.8 m AGL and at 609.6 m AGL at 51.44 meters per second. The FLIR Pro however, performs well even at altitudes above 609.6 m AGL at speeds of 51.44 meters per second and could be a useful low cost addition to current detection flights. The *u*TABI is the sensor that provides the most additional information on fire size and location and is thus the best higher cost option.

Our results indicate that forest fire detection has the potential to be ameliorated by the addition of this form of technology to current practices (Allison *et al*, 2016). Aerial infrared remote sensing at a tactical level, at moderate altitudes can allow for improved data acquisition and increased information about occurrence and development of fires and can help direct

suppression tactics. At an operational level, at low altitudes hotspot identification and suppression assessments are possible (Allison *et al*, 2016). The use of remote sensing in combination with suppression practices such as having remote sensing technologies onboard aircraft equipped for water bombing has been suggested to further increase the efficiency and utility of such technologies (Allison *et al*, 2016).

These results indicate that the use of aerial infrared remote sensing could improve current protocols. More precise data means that more fires will be accurately detected and that response times to those fires will be faster and more efficient. This is because we can interpret data with more accuracy when using data with more information. Therefore, although remote sensing is not yet standardized, this shows it would be a beneficial addition to current practices.

Future research direction:

Research in Alberta has been conducted in order to ameliorate current aerial protocols for fire detecting capabilities by providing more quantifiable information. These have explored ways to decrease air time, increase ability to deliver thermal information more rapidly and studying using fixed base applications in order to triangulate positions of smoke (Dutchak, 2006). This research could be further combined with our findings in order to allow for better prescription of services.

There is a gradual drying out of forest fuels during July and August with increasing fire danger (Joby *et al*, 2019). Frequent thunderstorms may occur then but little or no precipitation reaches the surface, so that frequent and severe lightning fires occur in both Canada and the United States. Technologies have been used for years to map weather and forecast potential storms (Joby *et al*, 2019). Since 2016, NASA has been using the Geostationary Lightning Mapper which is mounted on the GOES-16 satellite. This technology allows the collection of information which helps give insight to weather forecasters and emergency response teams before storms hit. Since lightning is linked to specific weather conditions, the area in which it has

the potential to strike is predictable (Joby *et al*, 2019). While we cannot predict individual strikes, forecasts for average lightning activity can be used to indicate the probability that lightning flash density will exceed a threshold for a particular area. This technology can even be useful up to a few days before a storm, meaning there is an opportunity for interference (Joby *et al*, 2019). Therefore, a combination of this type of technology with infrared remote sensing technologies such as those we have explored could allow for a more immediate fire detection system. Furthermore, the use of other forms of remote sensing have been theorized to be useful even in pre-fire conditions for fuel type mapping and in the prediction of high risk areas for fire development (Veraverbeke *et al*, 2018). This type of research could be crucial in the coming years due to increasing fire weather.

Chapter 5: Pre-fire biofuel characterization and identification of high risk areas using hyperspectral remote sensing technologies

Abstract:

Climate change is impacting our environment and health in several ways. The global warming of the planet has caused an increase in dryness. As a result, we see a decrease in overall plant health and function and an associated increase in the number and size of forest fires on a yearly basis. The drier the area of forest, the more at risk of fire it becomes. Current methodology for fire detection and suppression in Ontario, focuses on the detection of fires that are already burning and involves visual aerial detection of smoke by humans. Although this method has been beneficial for the management of effects of fires over the years, the idea of introducing pre-fire detection could provide important information which could enhance current detection practices. Thus, pre-fire high risk area identification was explored throughout this paper. The applicability of various vegetation indices in fire detection was examined. A preliminary study was done to determine the validity of the use of hyperspectral remote sensing in fire fuel characterization pre-fire for the determination of high risk areas. Our study demonstrated preliminary findings that this form of technology could be beneficial in the identification of high risk areas for ignition pre-fire and that further investigation is warranted.

Résumé:

Le réchauffement planétaire de la planète terre a plusieurs impacts sur l'environnement et notre santé. Ce réchauffement cause une diminution d'humidité et alors une diminution dans la santé de la végétation et dans leur fonctionnement. Ceci est donc lié à une augmentation dans le taux ainsi que la grandeur des feux de forêts à chaque année. La méthodologie courante pour la détection et suppression des feux concentre sur les feux actifs et compte sur la détection visuelle

de fumée par des observations aériennes. Cette méthode as améliorer la gestion des feux mais l'idée d'introduction de la détection de pré-feux pourrait nous provenir plusieurs nouvelles informations. Alors, l'identification de zones pré-feux à haute risque sera exploré le long de cet article. L'application de plusieurs indices de végétation a été explorée. Une étude préliminaire a été conduite afin de déterminer la validité des télédétecteurs hyperspectraux pour la characterization des combustibles pré-feux. Notre étude as demontrer des résultats préliminaires que cette sorte de technologie serait utile dans l'identification des zones à haute risque pour feu et qu'une enquête plus approfondie est justifiée.

Introduction

A branch of the Ministry of Natural Resources and Forestry (MNRF) called the Aviation, Forest Fire and Emergency Services (AFFES) program was developed in 1924 (AFFES, 2019). This is the world's longest operating, continuous flying, non-scheduled, government air service. AFFES is responsible for the management of natural disasters such as wildland fires, flooding and drought. AFFES performs all fire operations and organizes responses to incidents. Their goal is to optimize resource allocation, respond promptly and accurately to all reported incidents and make sure that the public as well as responders are safe (AFFES, 2019).

Two Regional Emergency Operations Centres (REOCs) make up Ontario's fire management program. The Northwest Region is comprised of Fort Frances, Kenora, Dryden, Thunder Bay, Red Lake, Sioux Lookout, and Geraldton. The Northeast Region is made up of Haliburton, Sudbury, Timmins, Chapleau, Wawa, and Cochrane. All sectors are monitored using aerial detection (AFFES, 2019).

Early detection of wildland fires is essential for control efforts and reduces the impacts of fires in terms of socioeconomic and suppression costs (Martell and Sun, 2008; Arienti *et al.* 2006; Cumming 2005; Hirsch *et al.* 1998; Kourtz 1994, 1987). The aerial detection program minimizes the impact of wildland fires by finding fires when they are smaller and more controllable and by providing more reliable information on fire size and position than found in public reports. It also contributes to risk management by making ignition sources clear and predicting fire behaviour as well as providing a way to monitor areas of concern. This coverage is only made possible by the fleet of 10 long-term contract aircraft which are primarily used for detection patrols (AFFES, 2019).

Two types of aerial detection are utilized in Ontario; the first being direct and the second being indirect. Direct detection involves events planned by fire managers for detection and reporting of fires. These are planned detection flights which actively search for fires in specific locations at specific times. Indirect detection involves detection by non-MNRF fire reporting. This is any passive detection or reporting done by the public or by industry or by suppression staff (AFFES, 2019; McFayden *et al.* 2019).

The method for detection currently being used in the aerial detection program is the use of observers on-board aircraft. The observer's duties involve scanning for fires by looking out of the windows in the airplane, reporting fires to the MNRF and completing the required paperwork. Although all observers are trained in the same way by the Ministry of Natural Resources and Forestry through a course called AV109 Aerial Detection for Pilots and Observers, relying on human eyesight is not as accurate as the implementation of new technologies could be (AFFES, 2019). Human vision is limited by several factors such as acuity, sensitivity to light, attention of the observer; the size, distance and intensity of the target and visibility factors such as haze, fog and dust clouds (Byram & Jemison, 1984). Therefore, this method of detection is prone to personal bias and human error.

An increase in the quantity and size of fires as a result of global warming is expected in the next century and this trend has already become obvious in some parts of the world (Woolford *et al.* 2014). These increases could hinder current protocols and render them less useful. This is especially true in Ontario, where the current detection infrastructure is not equipped to monitor the broadening area needing to be surveyed. The increase in quantity and size of fires would cause the current system to fail because of an inability to keep track of every individual fire as they start due to the limited number of detection personnel and aircraft available. Therefore, this

research examines the use of hyperspectral remote sensing technologies as an additional resource for current forest fire detection practices. The focus is on the use of these technologies for pre-fire characterization of fire fuels in order to determine areas at high risk for ignition. Ideally, this will allow better resource management.

Hyperspectral sensors detect wavelengths ranging from the visible, near-infrared and mid-infrared segments of the electromagnetic spectrum. These sensors allow differentiation between spectrally similar materials and provide accurate and detailed information that other sensors can not obtain (Shippert, 2004). This is because the broad range of wavelengths provided by these sensors allow differential absorption, transmission and reflectance of energy depending on the material being targeted and their biophysical and biochemical attributes such as its cellular structures and water content (Thenkabail & Lyon, 2016). Unlike multispectral sensors, that measure the reflectance, absorption and transmission of the earth's surface within a few wavelengths (up to 15 bands) with separations where no readings are taken, hyperspectral imagers measure the radiation in many (>100) discrete narrow bands (Hagen & Kudenov, 2013; Joseph *et al*, 2011). Therefore, each individual pixel appears as a spectrum, which is much more detailed (Shippert, 2004). The images produced from this form of remote sensing have been successfully used in fuel type mapping as well as in fire risk assessments in the pre-fire temporal phase in the fire disturbance continuum (Jain *et al*, 2004).

To date, the application of sensors in fire work has been limited by the technology being used. However, some findings such as the use of hyperspectral sensing in fuel type determination and quantification as well as in the determination of fire severity and recovery post-fire have been examined (Veraverbeke *et al*, 2018; Colombo *et al*, 2008; Jollineau & Howarth, 2008; Kokaly *et al*, 2007; Thenkabail *et al*, 2004; Lyon *et al*, 1998). Infrared sensing has also been

applied in order to determine fire temperatures as well as in the examination of active fires and in the determination of emission levels (Joseph *et al*, 2011).

Recent hyperspectral research has demonstrated the usefulness of this technology in pre- and post-fire conditions as well as during active fires. It is thought that the use of hyperspectral information in unison with data from multispectral or light detection and ranging (LIDAR) sensors could be extremely advantageous in forest fire research (Joseph *et al*, 2011). This is because a multi-source approach to increasing knowledge on fire fuel data and fire trends during active burning could allow earlier and more appropriate mitigation (Koetz *et al*, 2008).

Local weather dictates landscape-scale fire behaviour but biome-level fire behaviour is more appropriately linked to fire danger indices which are representations of daily synoptic weather patterns (Abatzoglou & Kolden, 2013). All fire danger indices are based on daily surface weather such as ignitability, spread rate and control difficulty. These indices also examine fuel consumption such as changes in fuel (live and dead plant material) moisture (Brown *et al*, 1991).

The present work deals with the application of hyperspectral sensing and the use of vegetation indices determined from the hyperspectral sensors tested, in pre-fire high risk biofuel identification. This was done by way of an airborne data study as well as a satellite data study. Using these technologies as additional information sources in fire detection could indicate high risk areas before a fire happens which would allow more efficient resource management and allocation. This chapter examines the use of hyperspectral remote sensing technologies for identifying changes in fire fuels by examining trends across a local sub area in Sudbury, Ontario, called Daisy Lake. This chapter also uses these methods to identify pre-fire risk across four separate areas, through imagery from before the fires happened, in areas which have been affected by fire.

Materials and Methods:

Study 1:

Selection of Datasets:

Sensors were flown on 20 June, 3 July, 8 July and 14 August 2019 (see Figures 1 and 2). These flights took off from the Greater Sudbury Airport and flew over a flight line near Daisy Lake. Daisy Lake is a lake in Greater Sudbury Ontario, Canada (NRC, 2016). It is in the Lake Huron drainage basin and is the source of the Whitefish River. The lake is approximately 3.2 kilometres by 0.3 kilometres, and lies at an elevation of 230 meters. It is located 0.7 kilometres south of the Ontario Highway 17. Surrounding Daisy Lake is the Daisy Lake Uplands Provincial Park. The park was officially designated by an amendment to the Ontario Provincial Parks Act in 2006. It is 620 hectares in size and is considered a non-operating park (NRC, 2016). This park serves to protect a recovering ecosystem polluted by the city's mining industry and is designated as a control area for ecological research. Unlike other parts of the city this area has been set aside in order to study the site's ability to recover on its own, without human intervention. The ecosystem is made up primarily of white birch trees, metal tolerant grasses, sedges, rock barrens and bog vegetation. This type of vegetation is strongly representative of the Sudbury area landscape which has a history of over 100 years of forestry, prospecting, mining, smelting and urbanization (MECP, 2016). Due to deforestation in the area heavy erosion of soils has taken place. The amount of disturbance of this area has affected biological diversity in the Daisy Lake Uplands Provincial Park and throughout Sudbury as a whole. Representative and special features in this area are the pioneer plant communities that have regrown in response to the disturbances previously mentioned. Previously, red pine and red oak grew in the dryer rock sites of this area and sugar maple and yellow birch grew in sites of deeper soil, however, these are no longer represented in the biodiversity of the area (MECP, 2016). The park topography is represented by

strongly broken, shallow and sandy till uplands. There is evidence of folding and partial metamorphism of the bedrock in this area and bedrock surfaces are blackened and etched from industrial atmospheric pollution (MECP, 2016). The area from which data was collected was an area primarily comprised of trees and barren rock (NRC, 2016).

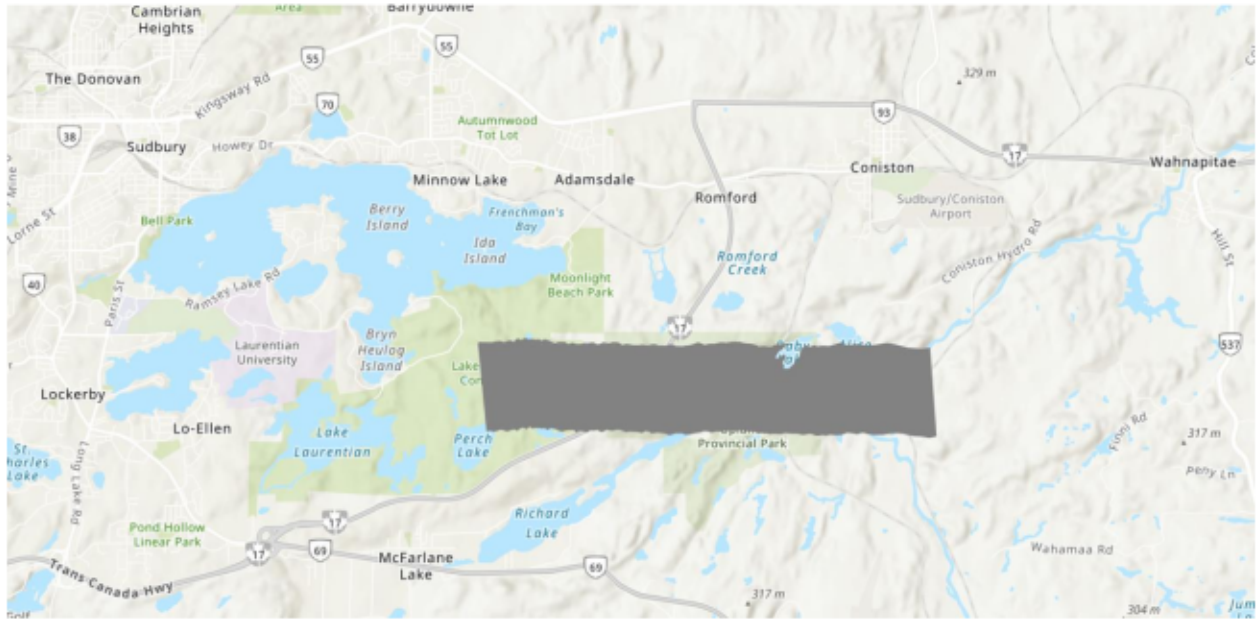


Figure 1. Daisy Lake Uplands Provincial Park flight line, Sudbury, Ontario, Canada. The grey area represents the area from which data was collected.

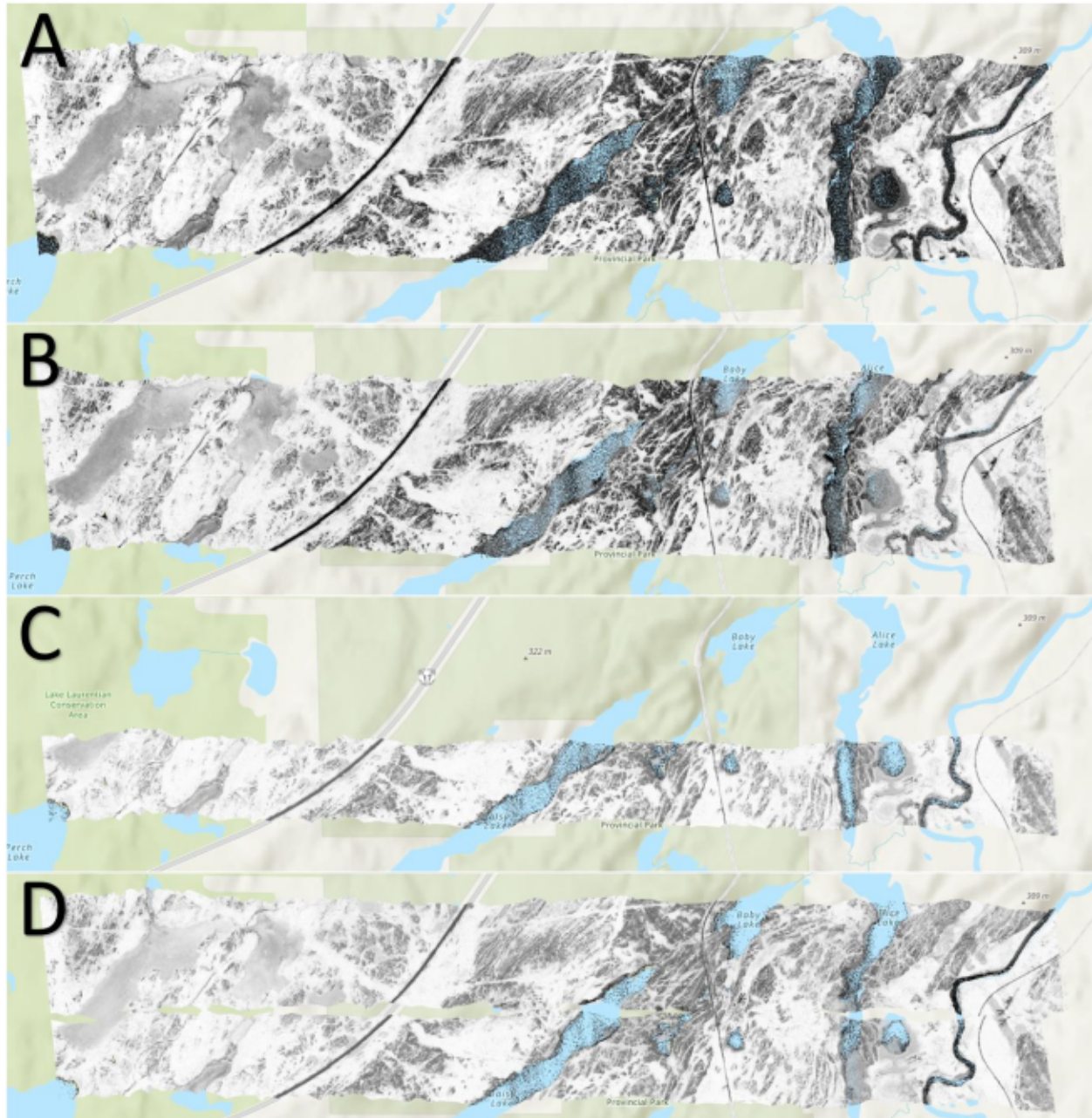


Figure 2. NDVI images of Daisy Lake demonstrating the overlapping data that was run through all vegetation indices. **A** represents data acquired June 20th. **B** represents data acquired July 3rd. **C** represents data acquired July 8th. **D** represents data acquired August 14th.

Sensor:

The sensor used in this study was the ITRES microCASI 1920 (*u*CASI), which is a portable air/ground hyperspectral VNIR imager. This sensor has a spectral coverage of 0.4-1.0 μm , 288 spectral channels, 1920 spatial imaging pixels and a 36.6° field of view (FOV). This sensor was

flown on an Aero Commander 500. This is a six-seat, high wing, fixed-wing, twin piston-engine aircraft.

Weather:

Average humidity percentages both three and seven days prior to data collection were calculated for each date flown.

Analysis:

Once aerial hyperspectral data was acquired for the site, the data was atmospherically corrected using the Fast Line-of-sight Atmospheric Analysis of Spectral Hypercubes (FLAASH) atmospheric correction code. The most representative data, in this case referring to data with the largest overlapping area among the different flight days, was selected. This overlapping data represented the same area across all dates. All selected data was then clipped to fit within the same geographical area. Multiple vegetation indices were then calculated using the hyperspectral data acquires, the index values for each pixel were then averaged and compared in order to identify if areas of higher risk for ignition could be identified and tracked according to preceding weather patterns.

Indices:

Forest Health:

The forest health tool is a spatial map which shows overall health of forested regions. It uses vegetation index categories such as: broadband and narrowband greenness; leaf pigments; canopy water content; and light use efficiency. These categories show the distribution of green vegetation, the concentration of carotenoids and anthocyanin pigments for stress levels, the concentration of water and forest growth rate respectively. This allows for an overall health estimation for a given area (Harris, 2020). The input scene is divided into nine classes from weakest or least healthy forest to healthiest.

Normalized Difference Vegetation Index (NDVI):

Chlorophyll absorbs visible light at 400 nm to 700 nm and the cell structure of leaves reflects near-infrared strongly from 700 nm to 1100 nm. Therefore, using visible and near-infrared data it is possible to determine if vegetation is live and green or not and to determine water stress. This information can then potentially be used in order to estimate fire danger. This index varies between -1 and 1, with free standing water showing very low positive or negative values as a result of its low reflectance in both spectral bands (Crippen, 1990; Rouse *et al*, 1973).

$$NDVI = \frac{(NIR - Red)}{(NIR + Red)}$$

Plant Senescence Reflectance Index (PSRI):

Senescence is defined as the condition or process of deterioration with age. As plants senesce they become higher risk fire fuels (McHugh & Gil, 2018). In many plants a preferential degradation of chlorophyll over carotenoids results in yellowing, therefore the use of a ratio between pigments can allow for the determination of senescence (Biswall 1995; Matile Ph Flash & Eller, 1991; Knee, 1988; Hendry *et al*, 1987; Knee, 1972; Chichester & Makayama, 1965). The estimation of chlorophyll has been shown to be possible when looking at reflectance in the green (550 nm) and red (700 nm) ranges of the visible spectrum (Gitelson and Merzlyak 1996, 1997). Thus, the Plant Senescence Reflectance Index (PSRI) uses the ratio of bulk carotenoids (alpha and beta) to chlorophyll. The value of this index ranges from -1 to 1 and the common range for green vegetation is -0.1 to 0.2 (Merzlyak *et al*, 1999).

$$PSRI = \frac{p_{680} - p_{500}}{p_{750}}$$

At around 750 nm fruit ripening and senescing leaves were seen for each species. At 500 nm reflectance is controlled by a combined absorption of Chlorophyll a, Chlorophyll b and

Carotenoids. At 680 nm this changes to Chlorophyll a absorption only. When there is a decrease in Chlorophyll the Carotenoid/Chlorophyll ratio increases. Thus, an increase in PSRI indicates that there is increased canopy stress (Carotenoids) (Merzlyak *et al*, 1999).

Study 2:

Selection of datasets:

An in depth analysis of several fires worldwide was conducted in order to be able to compare hyperspectral and multispectral analysis. Historical forest fire databases were explored for countries such as Canada, the United States, Greece and Russia. Search criteria focused on fires that had useable hyperspectral imagery within the area of the burn scar of the fire within one year before the fire occurred. These images needed to fit within the various satellite launch and decommission dates for the specific geographic location of the fire within those dates. They needed to have known burn scars with post-fire imagery and needed to be high quality images with low cloud cover, low pixilation, high visibility and no striping. Three hyperspectral databases were used in the identification of useable fire data. These include EO-1 Hyperion, Proba-1 Chris and AVIRIS.

Five fires were identified through this search. These include Cedar Fire in San Diego from 2003, a fire from 2012 in Bistrishko Branishte in Bulgaria, Rim Fire from California in 2013, King Fire from California in 2013 and the Mendocino Fire Complex from California in 2018. The Bulgaria fire was later removed from this analysis due to the image quality, noise and striping. See Figure 3. for datasets

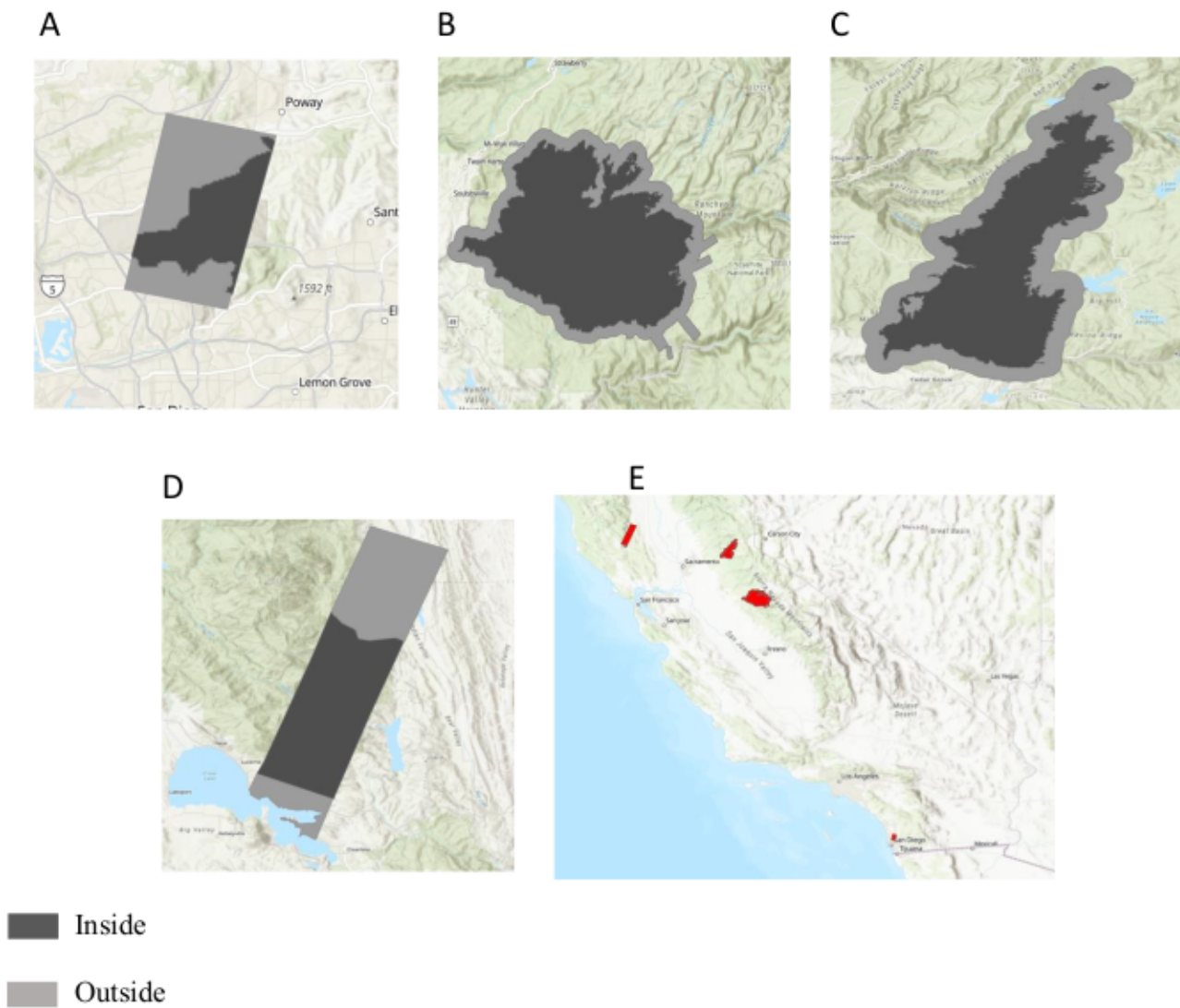


Figure 3. This figure represents the datasets used for study 2. The darker inner colour represents the area defined as inside. The lighter area represents the area defined as outside. **A** represents the data used for Cedar Fire. **B** represents the data used for Rim Fire. **C** represents the data used for King Fire. **D** represents the data used for Mendocino Fire Complex. **E** represents all four datasets in geographic relation to each other.

Cedar Fire:

Cedar Fire was a 273 246 acre (1 106 km²) wildland fire in San Diego County, California. This fire destroyed over 2200 homes and nearly 600 other properties, killed 15 people and caused non-fatal injuries to 113 people (CAL FIRE, 2019). This fire was started on October 25th, 2003 by a hunter who had gotten lost and wanted to be visible to rescuers (USDA, 2003). Once lit the hunter quickly lost control of the fire due to the heat, low humidity, low moisture content of surrounding vegetation as well as the wind conditions (USDA, 2003).

The fire started in the Cuyamaca Mountains in Cleveland National Forest with coordinates of 33.016667°N 116.683333°W. Within five and a half hours of the fire being reported it had grown in size to 5319 acres (USDA, 2003). To this day, this fire is one of the largest wildland fires in California history and actually ranks third in terms of size for the state (CAL FIRE, 2019).

The vegetation conditions recorded pre-fire and the week of the fire demonstrated historical maximums for fire potential hazards (USDA, 2003). Samples taken of old and new vegetation from Poser Mountain, San Diego County, California, on October 7th, 2003 showed averages of 49% and 55% respectively. Nighttime fine dead fuel moisture declined to 4 % and was even lower in the daytime. The National Fire Danger Rating System used indices such as Burning Index (BI), Energy Release Component (ERC) and 1000-Hour dead fuel moisture which were all at record measures of fire hazard (USDA, 2003).

Rim Fire:

Rim fire was a 257 314 acre (1041.31 km²) wildland fire in Sierra Nevada, in California in a remote canyon of Stanislaus National Forest. This was the third largest wildland fire in California's history. This fire started on August 17th, 2013 approximately 20 miles east of Sonora, California. Fire behaviour exhibited was high to extreme. The fire was caused by a

hunter's illegal fire and was responsible for destroying 11 residences, as well as three commercial buildings and 98 outbuildings (Lydersen *et al*, 2014). Several thousand people were evacuated as a result of this fire and a state of emergency was declared for the city of San Francisco (Staley, 2013). This was as a result of the fire causing damage to the power infrastructure serving the Bay Area, including shutting down two out of the three hydroelectric power plants (Peterson *et al*, 2015). On October 24th, 2013 the Rim Fire was declared contained. Hotspots on the inside of the perimeter of the fire continued to burn for a year before it was considered extinguished (Polivka *et al*, 2016).

King Fire:

King Fire was a 97 000 acre (390 km²) wildland fire in El Dorado County, California. This fire started on September 13th, 2014 near Pollock Pines, California to the east of Sacramento. The cause of this fire was arson, the fire was intentionally started. The King Fire destroyed 12 residences and 68 outbuildings and caused the evacuation of approximately 20 000 homes. It was the second largest wildland fire in the 2014 California wildland fire season. This fire was officially extinguished by October 31st 2014 (Stavros *et al*, 2018; Rocha & Xia, 2014).

Mendocino Fire Complex:

The Mendocino Fire Complex was a complex made up of two wildland fires that joined together to form a 459 123 acre (1858 km²) fire (CAL FIRE a, 2018). This Complex was comprised of the River Fire and the Ranch Fire in Mendocino County, Northern California, United States. This complex was the largest recorded fire complex in California causing over \$257 million (2018 USD). It destroyed 280 buildings and damaged 37 others. It also killed one firefighter and caused non-fatal injuries to four others. The Mendocino Complex also caused the evacuation of several local communities such as the city of Lakeport, communities of Kelseyville, Lucerne, Upper Lake, Nice, Saratoga Springs, Witter Springs, Potter Valley and Finley as well as parts of

Hopland and indigenous communities of Hopland Rancheria and Big Valley Rancheria (CAL FIRE b, 2018). The fires were started July 27th, 2018 and officially out November 7th, 2018.

The Ranch Fire alone burned 410 203 acres (1660 km²). This fire was originally reported at 12:05 pm on July 27th. This fire was reported to have been started by a farmer who had tried to seal an underground wasp nest by pounding a metal stake into it. The farmer inadvertently sparked the dry grass while hammering the metal stake into the ground (CAL FIRE a, 2018).

The Ranch fire became part of the Mendocino Complex when the River Fire started a few hours later. The complex started in the State Responsibility Area and burned through to Mendocino, Lake, Colusa and Glenn Counties. Once lit the farmer quickly lost control of the fire due to the heat, low humidity, low moisture content of surrounding vegetation and gusty winds (CAL FIRE a, 2018).

The River Fire was smaller and burned six miles north of Hopland, to the south of the Ranch Fire (CAL FIRE a, 2018). This fire was under control by August 13th according to local news, while the Ranch fire continued to burn for several months (Crauss, 2018). The cause of this fire is still under investigation.

Sensors:

Two hyperspectral sensors and two multispectral sensors were used.

EO-1 Hyperion:

The first hyperspectral dataset used in this study was obtained using the Earth Observing-1 (EO-1) Hyperion. Hyperion is an imaging spectrometer that records more than 200 wavelengths ranging from 0.357 to 2.576 micrometers with a 10 nm bandwidth. Hyperion is a push-broom sensor meaning it operates by collecting data following a specified path in a line. This data has a scene width of 7.7 kilometers and a standard length of 42 kilometers. The length can also be increased by an additional 185 kilometers. The pixel resolution of this sensor is of 30 m. This

sensor was attached to the EO-1, a decommissioned National Aeronautics and Space Administration (NASA) Earth observation satellite. EO-1 was launched 21 November 2000 by the U.S. Geological Survey (USGS) and NASA and was decommissioned 30 March 2017. The dataset used from this sensor is of San Diego, California from March 23rd, 2003. All details regarding this image are available in Table 1.

Table 1. EO-1 Hyperion dataset information

Data Set Attribute	Attribute Value
Entity ID	EO1H0400372003082110KV_SGS_01.
Cloud Cover	10% to 19% Cloud Cover
Orbit Path	41
Orbit Row	37
Target Path	40
Target Row	37
Station	SGS
Scene Start Time	2003:082:18:18:18.973
Scene Stop Time	2003:082:18:18:32.973
Sun Azimuth	139.18541
Sun Elevation	51.069536
Satellite Inclination	98.22
Look Angle	12.286
Center Latitude	32°37'16.58"N
Center Longitude	117°10'47.31"W
NW Corner Lat	33°01'08.71"N
NW Corner Long	117°06'28.97"W
NE Corner Lat	33°00'05.24"N
NE Corner Long	117°01'27.13"W
SE Corner Lat	32°13'24.70"N
SE Corner Long	117°15'06.90"W
SW Corner Lat	32°14'27.66"N
SW Corner Long	117°20'06.23"W

AVIRIS:

The second, third and fourth hyperspectral datasets used in this study were obtained using

Airborne Visible/Infrared Imaging Spectrometer (AVIRIS). AVIRIS is an imaging spectrometer developed at the Jet Propulsion Laboratory at NASA. This sensor delivers calibrated images in

224 contiguous wavelengths ranging from 400 to 2500 nanometers. Using four spectrometers and scanning optics it is able to image a 614 pixel swath simultaneously from each of the 224 bands. AVIRIS is not attached to a satellite but is instead flown as a high altitude sensor from aircrafts such as ER-2-AFRC, Proteus, Twin Otter and WB-57-JSC. AVIRIS has been flown over North America, Europe and portions of South America but concentrates mostly on data acquisition for the United States.

The first and second datasets used from this sensor were sourced from a secondary government website - these files were preprocessed and the original unprocessed files were not readily available (Stavros *et al.*, 2016). The first dataset represents a remote canyon in Stanislaus National Forest, California from June 26th, 2013. The second dataset represents El Dorado County, California on September 19th, 2013.

The third dataset used from this sensor is of Mendocino, California from June 12th, 2018. All available information on this flight is located in Table 2 and was sourced directly from the AVIRIS government website.

Table 2. AVIRIS dataset information

Data Set Attribute	Attribute Value
Entity ID	f180612t01p00r08
Site Name	HyspIRI_3_line12 (orthorectified)
Start Lat	42.9253753
Start Lon	-120.7521843
Stop Lat	37.6873814
Stop Lon	-123.3472464
Start GMT	1918
Stop GMT	2011
Comments	Flight South to North

Landsat 7:

Landsat 7 was launched on April 15th, 1999 as the seventh satellite of the Landsat Program. Its mission was to provide updated and high quality cloud-free imagery. This satellite was

developed by Lockheed Martin Space Systems and operated by USGS and NASA. Its design enables it to take 532 images per day with a panchromatic band of 15 m spatial resolution. It also can detect visible, near-infrared and mid-infrared wavelengths with 30 m spatial resolution, and thermal wavelengths with 60 m resolution. On May 31st, 2003 the Scan Line Corrector (SLC) in the ETM+ instrument failed. The role of the SLC is to correct for the forward motion of the spacecraft. Therefore, approximately 22% of the data from each image collected after the date of the SLC failure is missing. For this reason, only images taken prior to the SLC failure were considered during this research.

The image used from this sensor is the multispectral image of the Cedar Fire, San Diego County, California, United States. This was used in order to determine the boundary of the burn scar. The image was collected on May 19th, 2003. All data associated to the image is available in Table 3.

Table 3. Landsat 7 dataset information

Data Set Attribute	Attribute Value
Entity ID	LE07_L1TP_040037_20030519_20160928_01_T1
Land Cloud Cover	1%
Center Latitude	33°09'32.40"N
Center Longitude	117°13'58.80"W
NW Corner Lat	34°06'55.80"N
NW Corner Long	118°01'43.32"W
NE Corner Lat	33°49'13.44"N
NE Corner Long	115°59'28.68"W
SE Corner Lat	32°29'07.80"N
SE Corner Long	118°27'23.76"W
SW Corner Lat	32°11'44.88"N
SW Corner Long	116°27'22.32"W

Landsat 8:

Landsat 8 is an American Earth observation satellite; it was launched February 11th, 2013. This satellite provides moderate-resolution imagery from 15 to 100 metre resolution. It operates in visible, near-infrared, short wave infrared and thermal infrared spectrums. It captures over 700 images per day. Two images from this sensor were used for the Mendocino Fire Complex. The

first image (Table 4) was collected July 17th, 2018 and represents Mendocino before the fire. The second image (Table 5) was collected October 30th, 2018 and represents Mendocino after the fire. These were used in order to determine the boundary of the burn scar.

Table 4. Landsat 8 Mendocino Fire Complex dataset information before fire

Data Set Attribute	Attribute Value
Entity ID	LC08_L1TP_045033_20180710_20180717_01_T1
Land Cloud Cover	0.1%
Center Latitude	38°54'16.49"N
Center Longitude	123°12'00.79"W
NW Corner Lat	39°57'27.90"N
NW Corner Long	124°01'08.76"W
NE Corner Lat	39°33'11.27"N
NE Corner Long	121°51'15.12"W
SE Corner Lat	38°14'21.98"N
SE Corner Long	124°31'25.03"W
SW Corner Lat	37°50'11.62"N
SW Corner Long	122°24'36.65"W

Table 5. Landsat 8 Mendocino Fire Complex dataset information after fire

Data Set Attribute	Attribute Value
Entity ID	LC08_L1TP_045033_20181030_20181115_01_T1
Land Cloud Cover	0.2%
Center Latitude	38°54'15.16"N
Center Longitude	123°13'46.20"W
NW Corner Lat	39°57'25.78"N
NW Corner Long	124°02'55.50"W
NE Corner Lat	39°33'11.02"N
NE Corner Long	121°53'01.46"W
SE Corner Lat	38°14'19.72"N
SE Corner Long	124°33'09.47"W
SW Corner Lat	37°50'11.11"N
SW Corner Long	122°26'20.69"W

Analysis:

Pre-fire imagery was assessed and classified in terms of what burned (Inside) and what did not burn (Outside). The data from the Rim Fire and the King Fire were sourced from a secondary government website, and as a result two treatments of the data exist.

Treatment 1: Cedar Fire and Mendocino Fire Complex:

Firstly, the data from Cedar Fire and the Mendocino Complex Fire were atmospherically corrected using the Fast Line-of-sight Atmospheric Analysis of Spectral Hypercubes (FLAASH) atmospheric correction code. The area of the burn scar within the hyperspectral image was measured in km² and an equal sized area outside of the burn scar was selected to represent the outside vegetation. The inside and outside of the burn scar were identified and defined on the hyperspectral images from before the fires occurred. The data was then run through multiple indices for both the areas within and outside of the fire. The index values for each pixel were then averaged for both the inside and the outside of the fires and this data was then compared.

Treatment 2: Rim and King Fires:

The processed data was acquired. The inside of the perimeter of the fire was separated from the outside buffer area. The buffer area represents a 2-km buffer around the fire boundary of the respective fire area. In this case, the data available had already been run through the various indices using topographically, atmospherically-corrected, and georectified data. The index values for each pixel were then averaged for both the inside and the outside of the fires and this data was then compared.

Indices:

Moisture Stress Index (MSI):

This index is a reflectance measurement that is sensitive to increasing leaf water content. As water content in canopies increases, absorption around 1599 nm increases. Absorption at 819 nm is unaffected by water content and is therefore used as reference. The value of this index ranges

from 0 to more than 3 and the common range for green vegetation is from 0.4 to 2 (Vogelmann & Rock, 1985).

$$MSI = \frac{p_{1599}}{p_{819}}$$

Please see section 1.3 for the rest of the indices as the same ones were used. FH was not used for the Rim and King fires as this data was not available.

Results:

Study 1:

Index values were run through a repeated measures analysis of variance in order to detect any overall differences between the dates that were flown.

Forest health (FH):

The FH analysis revealed that all dates were significantly different from each other ($F_{(3, 43946880)} = 265243.976, p < .001$). The FH values for June 20th were significantly higher than those from July 3rd ($p < .001$) and July 8th ($p < .001$). This analysis also revealed that June 20th had a significantly lower FH than that of August 14th ($p < .001$). The FH values for July 3rd were significantly lower than all other dates ($p < .001$). July 8th FH values were higher than July 3rd ($p < .001$) and lower than those of June 20th ($p < .001$) and August 14th ($p < .001$). FH values for August 14th were higher than all other values ($p < .001$).

Normalized Difference Vegetation Index (NDVI):

The NDVI analysis revealed that all dates were significantly different from each other ($F_{(3, 48397281)} = 29846.632, p < .001$). The NDVI values for June 20th were significantly lower than all other dates. July 3rd values were significantly higher than all other dates ($p < .001$). The NDVI values for July 8th were higher than those from June 20th ($p < .001$) and August 14th ($p < .001$). July 8th NDVI values are significantly lower than those from July 3rd ($p < .001$). August 14th

NDVI values were higher than those from June 20th ($p < .001$) and lower than those from July 3rd ($p < .001$) and July 8th ($p < .001$).

Plant Senescence Reflectance Index (PSRI):

The PSRI analysis revealed that all dates were significantly different from each other ($F_{(3, 49057935)} = 12970.020$, $p < .001$). June 20th PSRI values were higher than both July 3rd ($p < .001$) and July 8th ($p < .001$). June 20th values were lower than August 14th ($p < .001$). July 3rd values were significantly higher than July 8th ($p < .001$) and significantly lower than June 20th ($p < .001$) and August 14th ($p < .001$). July 8th values were significantly lower than all other dates ($p < .001$). August 14th PSRI values were significantly higher than all other dates ($p < .001$).

Weather:

A paired samples t test was run in order to compare the means between the humidity levels at 3 and 7 days prior to the flight dates. This analysis revealed that the mean humidity 7 days prior to the flight dates was always significantly higher than the mean humidity 3 days prior ($t(3) = 28.041$, $p < .001$). The means for each flight date can be found in table 6.

FH:

A multiple linear regression was calculated using a stepwise method to predict FH based on humidity percentage, the mean humidity percentage three days prior to data collection and 7 days prior to data collection were used as independent variables. A significant regression equation was found ($F_{(2, 96763828)} = 130417.063$, $p < .001$), with an R^2 of 0.003. The predicted FH values are equal to $4.680 - .007 + .317$, where FH increased by .317 with each percent of humidity.

NDVI:

A multiple linear regression was calculated using a stepwise method to predict NDVI based on humidity percentage, the mean humidity percentage three days prior to data collection and 7 days prior to data collection were used as independent variables. A significant regression equation was

found ($F_{(2, 48397281)} = 42017.925, p < .001$), with an R^2 of 0.002. The predicted NDVI values are equal to $.372 + .041 - .063$, where NDVI decreased by .063 with each percent of humidity.

PSRI:

A multiple linear regression was calculated using a stepwise method to predict PSRI based on humidity percentage, the mean humidity percentage three days prior to data collection and 7 days prior to data collection were used as independent variables. A significant regression equation was found ($F_{(2, 49057935)} = 14909.717, p < .001$), with an R^2 of 0.001. The predicted PSRI values are equal to $.344 - .024 + .020$, where PSRI increased by .020 with each percent of humidity.

Table 6. Mean humidity %

Dates	Humidity % 3 Days Prior	Humidity % 7 Days prior
June 20 th	65.76	73.31
July 3 rd	70.01	77.62
July 8 th	68.67	75.4
August 14 th	64.25	70.92

Study 2:

An independent samples t test was done to compare the means between the inside and outside of the fires for each index in order to determine whether these areas were significantly different from each other. The mean values can be found in table 7.

Cedar Fire:

The inside and outside areas were significantly different from each other for each index. The means inside of the fire area were significantly higher for the FH ($t(126187) = 131.937, p < .001$), MSI ($t(126187) = 10.177, p < .001$) and NDVI ($t(126187) = 126.892, p < .001$) indices. The mean outside of the fire area was significantly higher for the PSRI ($t(126179) = -5.467, p < .001$) index.

Rim Fire:

The inside and outside areas were significantly different from each other for each index. The mean inside of the fire area was significantly higher for NDVI ($t(2552513) = 44.005, p < .001$).

The means outside of the fire area were significantly higher for both the PSRI ($t(437278) = -55.277, p < .001$) and MSI ($t(3518479) = -533.587, p < .001$) indices.

King Fire:

The inside and outside areas were significantly different from each other for each index. The mean inside of the fire area was significantly higher for NDVI ($t(3171339) = 304.808, p < .001$).

The means outside of the fire area were significantly higher for both the PSRI ($t(157092) = -16.14, p < .001$) and MSI ($t(3168940) = -173.25, p < .001$) indices.

Mendocino Fire Complex:

The inside and outside areas were significantly different from each other for each index. The means inside of the fire area were significantly higher for the FH ($t(2630735) = -807.750, p < .001$), MSI ($t(2628776) = 297.388, p < .001$) and NDVI ($t(2628776) = -297.388, p < .001$) indices. The mean outside of the fire area was significantly higher for the PSRI ($t(2628767) = -48.540, p < .001$) index.

Table 7. Mean index values inside and outside of burn scar areas for Cedar Fire, Mendocino Fire Complex, King Fire and Rim Fire

	Cedar Fire		Mendocino Fire Complex		King Fire		Rim Fire	
Index	Inside	Outside	Inside	Outside	Inside	Outside	Inside	Outside
FH	6.32	4.39	5.13	7.02	N/A	N/A	N/A	N/A
MSI	0.531	0.347	0.641	0.356	0.481	0.540	0.626	0.837
NDVI	0.531	0.347	0.356	0.641	0.779	0.540	0.703	0.007
PSRI	0.137	0.164	0.031	0.212	0.309	0.320	0.216	0.224

Discussion:

The use of hyperspectral sensors in forest fire applications has been limited thus far (Joseph *et al*, 2011). Due to the unpredictability of fires, data collection is complicated and the majority of research has been completed using laboratory measurements as opposed to field measurements (Allison *et al*, 2006). This being said, the data available for such research is also limited. This is

certainly true in the case of hyperspectral data. Similarly, no general forest fire database exists for the purpose of locating fires that demonstrate specific criteria for the purpose of research. However, this is a pilot project and the trends discovered through out this project are essential for the development of modifications for larger scale application and further research.

Study 1:

Forest health (FH):

The results for FH demonstrate that all dates were significantly different from each other. In terms of health in accordance with the Forest Health analysis, results demonstrated that August 14th was significantly healthier than all other dates. This was followed by June 20th, July 8th and July 3rd respectively.

Normalized Difference Vegetation Index (NDVI):

The results for NDVI demonstrate that all dates were significantly different from each other. In terms of health in accordance with the Normalized Difference Vegetation Index analysis, results demonstrated that July 3rd was significantly healthier than all other dates. This was followed by July 8th, August 14th and June 20th respectively.

Plant Senescence Reflectance Index (PSRI):

The results for PSRI demonstrate that all dates were significantly different from each other. In terms of health in accordance with the Plant Senescence Reflectance Index analysis, results demonstrated that July 8th was significantly healthier than all other dates. This was followed by July 3rd, June 20th and August 14th respectively.

Weather:

The results for weather in terms of percentage of humidity, demonstrate that all dates were significantly different from each other. In terms of health in accordance with humidity, results demonstrated that July 3rd was significantly more humid than all other dates. This was followed by July 8th, June 20th and August 14th respectively.

Overall trends:

According to the results, none of the indices used in this study demonstrated the same trends as the humidity. The hypothesis was that the humidity would be a major influence in the determination of health for each index as seen in other studies (Ozyavuz *et al*, 2015; Funk & Brown, 2006; Meyers *et al*, 1970). However, according to our data all indices demonstrated significantly different data for each date therefore demonstrating their individual abilities to differentiate according to their respective criteria. This means that although we did not see a unanimous result of which date seems the healthiest, each index was capable of sequentially scoring the data from separate dates.

Furthermore, if we group the data from June 20th and August 14th and compare it to the grouped data from July 3rd and 8th we see that the July group is higher in the sequence than the June and August group for NDVI and PSRI. This would mean that the July group is rated healthier than the June and August group overall for those two indices. Likewise, the humidity analysis ranks the July group higher than the June and August group in terms of humidity. Taking this into account, we can see that our data is following a similar trend to the humidity analysis which leads us to believe that our findings are in accordance with the hypothesis that humidity would be a major influence in the determination of health.

Additionally, these findings would indicate that if humidity is a predictor of health, FH does not seem to be a good indicator of high risk areas. Necessarily, this indicates that NDVI and PSRI would not be good predictors of FH.

Limitations:

Although we were able to see trends in our grouped data, limitations do exist in this study. Humidity is one of the main components responsible for the characterization of fire fuels as high risk for ignition (Schroeder & Buck, 1970). Our weather analysis on percentage of humidity

shows a significant correlation to the indices however, these results are not as significant as we expected. This can be explained based on the fact that the humidity readings are showing relative humidity for Greater Sudbury versus the local humidity in the exact area of Daisy Lake being monitored. Thus, it would be important to take local readings in future research.

Furthermore, our research focuses on short term changes in humidity from 3 and 7 days prior to our data collection which indicates that the changes being reported are most likely related to an atmospheric effect and may not be representative of the plant physiology. In order to see the effect of humidity on the health and function of plants and not on the atmospheric level, atmospheric corrections were done using FLAASH. This form of correction may however, not have been sufficient enough to counter the effects of temperature and humidity on the transmission of wavelengths (Villars & Weisskopf, 1954). Plant acclimation to humidity varies depending on the type of vegetation being monitored and on the hydro-climate of the area being studied, therefore, the small time frame being used for comparison may not be fully appropriate to represent changes in plant health and function (Cowles *et al*, 2018; Pappas *et al*, 2018; Amiro *et al*, 2006).

Study 2:

Cedar Fire and Mendocino Fire Complex:

The trends for all indices (FH, MSI, NDVI and PSRI) for both of these fires were the same. For both fires, the results demonstrated that the inside and outside areas were significantly different from each other. In terms of health, FH, NDVI and PSRI indicated that the inside vegetation was healthier than the outside vegetation. However, the MSI index indicated that the inside area demonstrated a higher stress level and was therefore, less healthy than the outside area.

Rim Fire and King Fire:

The trends for all indices (MSI, NDVI and PSRI) for both of these fires were the same. For both fires, the results demonstrated that the inside and outside areas were significantly different from each other. In terms of health, MSI, NDVI and PSRI indicated that the inside vegetation was healthier than the outside vegetation.

Overall Trends:

Two treatments of the data exist and we see that the trends are representative of the treatments. Thus, we see that in the case of the preprocessed data (Rim Fire and King Fire) sourced from a secondary government website we are unable to prove the hypothesis that by using this set of indices we are capable of identifying areas at high risk for fires. However, by using our methodology from the material and methods section 2.3 Analysis for Cedar Fire and Mendocino Fire Complex, we were able to see a high risk area in the pre-fire data.

The composition and moisture content of forest vegetation is a factor in the probability of ignition (Wotton & Martell, 2005). When vegetation is dry and wind is sufficient, fires can spread almost immediately and become active surface or crown fires. If surface fuels are damp and deeper underground organic layers are dry, we see “holdover” fires which smoulder in the deeper layers until surface fuels dry or until fuel is no longer available (Martell & Sun, 2008). Atmospheric moisture also has a direct effect on flammability and indirect effects on fire behaviour (Schroeder & Buck, 1970). Not only does moisture affect the dryness of potential fire fuels, it also affects surface temperature by controlling radiation in its vapour state and by reflecting and radiating in its condensed cloud form.

Water vapor in the air can come from three places - evaporation from water bodies, evaporation from soil, and transpiration of plants. This means that in a dry environment, vegetation is drier because the moisture content is transpired by the plants and taken back into the atmosphere. This

means that these plants are more likely to become fire fuels (Schroeder & Buck, 1970). This illustrates the influence that moisture content has on forest fires both on the surface and in deeper organic layers. Our research highlighted the importance of moisture in prefire fuel characterization as MSI was the only index that was capable of qualifying the inside area for both Cedar Fire and the Mendocino Fire Complex data as less healthy than the outside area which did not burn. This being said, for our raw datasets, MSI was the only index with the ability to consistently indicate an area at higher risk for ignition before the fire happened.

Limitations:

Our study allowed us to see preliminary findings on the application of hyperspectral remote sensing technologies for use in fire fuel characterization and in the identification of high risk areas for ignition. However, many limitations exist related to our study.

Firstly, as mentioned in the limitations section of study 1, environmental conditions such as temperature, humidity and differences in the biodiversity of land cover can impact findings in this field of study (Schroeder & Buck, 1970). Environmental conditions have an impact on plant physiology but also on the transmission of wavelengths (Villars & Weisskopf, 1954). Our atmospheric corrections using FLAASH may not have been sufficient enough to eliminate atmospheric effects on our data. These environmental conditions need to be monitored in future studies and it is important that this data be representative of the precise area being studied. Weather data from the specific area being researched would improve the validity of any findings. It is however important to understand that this study is based on data pre-fire and that data collection was not done specifically for the purpose of determining areas at high risk of ignition. The data used throughout this study was selected because it coincided with areas which happened to ignite, therefore some information which could be useful for the elimination of

atmospheric or environmental effects was not collected, this includes things like wind speed, fire weather, environmental conditions, shadow conditions, etc. This means that unlike in a staged event like in study 1, we are reliant on data which is acquired for other purposes and as such we are limited in what we are able to control for.

Our research focuses on the averages of mixed land cover which should be corrected for in future research. This is because different land covers may not be comparable, if for example a wetland is being compared to a forested area, the results for high risk areas for ignition would be biased by the water content in the wetland (Herold *et al*, 2008). Using a land cover classification system would allow us to separate areas of similar biodiversity and the comparison between the grouped areas would improve the validity of any findings (Anderson, 1976). Furthermore, using randomized points from data separated into vegetation types would allow for the correction of unknowns such as the topography, hydrology, age of vegetation, species, etc (Rodriguez-Galiano *et al*, 2012).

Another limitation of our study is the possible lag between plant physiology and acclimation to the environmental conditions in the areas being analysed. The hyperspectral data used in this study is pre-fire imagery from within one year before the fire happened. There are variations in the timeframe from which the data was acquired and when the fire happened. For example, the data used from the Rim Fire was collected 1.5 months before the fire started. However, the data from the King Fire was collected one full year before the fire started. The impact of the data acquired closer to the time of the fire is more representative of the vegetation health at the time of the fire than data acquired several months before the fire even happened. Therefore, it may be necessary to change the timeframe criteria for dataset collection as older data may not be representative. The criteria for future research would need to be based on plant acclimation

studies in order to represent changes in plant health and function (Cowles *et al*, 2018; Pappas *et al*, 2018; Amiro *et al*, 2006).

Finally, the small sample size in this study due to the difficulties related to finding data which fit the criteria of timeframe, image quality and cover the area of the burn scar pre-fire limits our ability to determine trends in the data. There is also variation due to the use of different hyperspectral sensors which function at different altitudes and have different pixel resolutions. This could impact the results as the data from one sensor could be of higher quality than another dataset and could make comparisons between the two difficult (Townsend & Foster, 2002).

Conclusion:

Our data suggests that the indices used in our research were capable of differentiating areas of lower vegetation quality from areas of healthier vegetation with some limitations. While these indices were capable of differentiating values that represented significantly differentiated data, our results did not show the expected consistency across indices. It is important to note that we were not testing the validity of these indices, rather testing their use in forest fire research.

In the first study we can conclude that although we can not see an exact replica of the pattern of humidity among the indices, we are able to see a trend emerge when the dates are grouped. This indicates that further investigation into this trend is warranted. Therefore, the second study was conducted.

In the second study we can see a difference between the preprocessed data treatment and the original raw data treatment. The results demonstrate that when using our methodology (raw data treatment) with the MSI index we are able to see an area at high risk before a fire happens. This is important information that could be used in further research and in current sensor related protocols for fuel source mapping for forest fires and the forestry industry.

The two biggest influences on fire behaviour are wind and fuel moisture (Schroeder & Buck, 1970). Therefore, it would be possible to determine where high-risk areas exist by use of remote sensing which would allow for better coordination of firefighting practices and resource allocation.

Future research:

Research on forest fire danger rating has been a work in progress in Canada since 1928. Several different systems have been created over time and thus several different indices exist (Van Wagner, 1974). The use of these indices in protocol development for fuel type mapping pre-fire is novel and seems promising. Our research suggests that the direction that future research should be taking is examining indices related to water content and humidity. One index that could be introduced in a similar fashion is the Water Band Index (WBI). The WBI is a reflectance measurement that looks at water content in the canopy and should be compared to our findings with MSI.

Research has been conducted on treatments that can be done on forested areas in order to minimise the risks of ignition. These involve removing undergrowth, creating dozer lines, mechanical thinning of trees and the use of prescribed burnings (USDA, 2013). The results demonstrate that in general the treated areas see reduced fire intensity in comparison to surrounding untreated areas. Thus, future research could concentrate on the implementation of these treatments in prevention policies which could be reinforced in areas at high risk.

Finally, future research should focus on the implementation of storm tracking in unison with remote sensing in order to be able to better predict areas at high risk for forest fire ignition. Lightning is the only known natural source of ignition for fires and the probability that lightning causes a sustainable ignition in a forested area has been researched (Wotton, 2005). Similarly, research has been conducted in order to develop systems better able to track where lightning will

hit (Ullah *et al*, 2019). This research in combination with our findings should be explored in order to create the best prediction model.

Chapter 6: Conclusion

In this thesis, several studies were conducted in order to assess the applicability of the implementation of remote sensing technologies for potential use in forest fire management protocols.

The quantity of forest fires is increasing due to climate change. With this, the health of both humans and of the environment are being affected. We know that smoke inhalation is one of the main concerns for human health and that the effects are associated to the components being burned by the fire. In terms of the environment, the main concerns include effects on air, soil, vegetation and water. Current methodology lacks the ability to quickly and accurately acquire data on fires that are burning. The sooner a fire is detected, the sooner mitigation strategies can be applied and thus, the smaller the effect on health.

Chapter 4, concentrates on the application of infrared remote sensing technologies on early mitigation of forest fires. Thanks to the results from this chapter, we can conclude that forest fire detection has the potential to be ameliorated by the use of this form of remote sensing technologies. Our results indicate that each sensor has its limitations and that the abilities of the sensors are limited by altitude. Our findings indicate that each of the sensors tested could be useful at different altitudes and that the lowest cost addition to current methodology would be the FLIR Duo Pro R.

Chapter 5, concentrated on the application of hyperspectral remote sensing technologies on pre-fire bio-fuel characterization for the identification of areas at high risk for forest fires. Our findings allow us to conclude that this form of remote sensing is also a valuable tool that could be used to ameliorate current methodology. Our results suggest that we were able to differentiate areas of higher and lower vegetation quality. Our data highlights the importance of fuel moisture

in the probability of ignition. Finally, we conclude that the Moisture Stress Index can be used to determine areas of high risk.

Overall, we can conclude that the implementation of remote sensing technologies into standard forest fire detection and monitoring protocols would be beneficial. It would allow for more detailed and accurate information on early fires and on areas at higher risk for ignition.

References:

- Abatzoglou, J. T., & Kolden, C. A. (2013). Relationships between climate and macroscale area burned in the western United States. *International Journal of Wildland Fire*, 22(7), 1003-1020.
- Adelberger, E. G., Heckel, B. R., & Nelson, A. E. (2003). Tests of the gravitational inverse-square law. *Annual Review of Nuclear and Particle Science*, 53(1), 77-121.
- AFFES Ministry of Natural Resources and Forestry Canada. (2019). AV109 *Aerial Detection for Pilots & Observers Student Reference Notes*. AFFES Publication P00457.
- Alaluusua, S., Lukinmaa, P. L., Vartiainen, T., Partanen, M., Torppa, J., & Tuomisto, J. (1996). Polychlorinated dibenzo-p-dioxins and dibenzofurans via mother's milk may cause developmental defects in the child's teeth. *Environmental Toxicology and Pharmacology*, 1(3), 193-197.
- Allison, R. S., Johnston, J. M., Craig, G., & Jennings, S. (2016). Airborne optical and thermal remote sensing for wildfire detection and monitoring. *Sensors*, 16(8), 1310.
- Ambrosia, V.G.; Wegener, S.; Zajkowski, T.; Sullivan, D.V.; Buechel, S.; Enomoto, F.; Lobitz, B.; Johan, S.; Brass, J.; Hinkley, E. (2011) The Ikhana unmanned airborne system (UAS) western states fire imaging missions: From concept to reality (2006–2010). *Geocarto Int.* 2011, 26, 85–101.
- Amiro, B. D., Stocks, B. J., Alexander, M. E., Flannigan, M. D., & Wotton, B. M. (2001). Fire, climate change, carbon and fuel management in the Canadian boreal forest. *International Journal of Wildland Fire*, 10(4), 405-413.
- Amiro, B. D., Barr, A. G., Black, T. A., Iwashita, H., Kljun, N., McCaughey, J. H., ... & Saigusa, N. (2006). Carbon, energy and water fluxes at mature and disturbed forest sites, Saskatchewan, Canada. *Agricultural and forest meteorology*, 136(3-4), 237-251.

- Anderson, J. R. (1976). *A land use and land cover classification system for use with remote sensor data* (Vol. 964). US Government Printing Office. Arienti, M.C.; Cumming, S.G.; Boutin, S. (2006). Empirical models of forest fire initial attack success probabilities: The effects of fuels, anthropogenic linear features, fire weather, and management. *Can. J. For. Res.* 2006, 36, 3155–3166.
- Arrue, B. C., Ollero, A., & De Dios, J. M. (2000). An intelligent system for false alarm reduction in infrared forest-fire detection. *IEEE Intelligent Systems and Their Applications*, 15(3), 64-73.
- Biswal, B. (1995). Carotenoid catabolism during leaf senescence and its control by light. *Journal of Photochemistry and Photobiology B: Biology*, 30(1), 3-13.
- Bonazountas, M., Kallidromitou, D., Kassomenos, P., and Passa, N. (2007). A decision support system for managing forest fire casualties. *J. Environ. Manage.* 84(4):412–418.
- Bowman, D. M., & Johnston, F. H. (2005). Wildfire smoke, fire management, and human health. *EcoHealth*, 2(1), 76-80.
- Brown, J. K., Reinhardt, E. D., & Fischer, W. C. (1991). Predicting duff and woody fuel consumption in northern Idaho prescribed fires. *Forest Science*, 37(6), 1550-1566.
- Burke, M. P., Hogue, T. S., Ferreira, M., Mendez, C. B., Navarro, B., Lopez, S., & Jay, J. A. (2010). The effect of wildfire on soil mercury concentrations in Southern California watersheds. *Water, Air, & Soil Pollution*, 212(1-4), 369-385.
- Byram, G.M.; Jemison, G.M. (1948). Some Principles of Visibility and Their Application to Forest Fire Detection; *Department of Agriculture*.

- CAL FIRE a (2018). Ranch Incident Investigation Report. California, United States: California Department of Forestry and Fire Protection.
- CAL FIRE b (2018). Mandatory Evacuation For the Mendocino Complex. California, United States: California Department of Forestry and Fire Protection.
- CAL FIRE (2019). Top 20 Deadliest California Wildfires. California, United States: California Department of Forestry and Fire Protection.
- Campbell, J. B., & Wynne, R. H. (2011). *Introduction to remote sensing*. Guilford Press.
- Certini, G. (2005). Effects of fire on properties of forest soils: a review. *Oecologia*, 143(1), 1-10.
- Chang, C. I. (2003). Hyperspectral imaging: techniques for spectral detection and classification (Vol. 1). *Springer Science & Business Media*.
- Chichester, C. O., & Nakayama, T. O. M. (1965). Pigment changes in senescent and stored tissue. *Chemistry and biochemistry of plant pigments*, 439, 458.
- Colombo, R., Meroni, M., Marchesi, A., Busetto, L., Rossini, M., Giardino, C., & Panigada, C. (2008). Estimation of leaf and canopy water content in poplar plantations by means of hyperspectral indices and inverse modeling. *Remote sensing of environment*, 112(4), 1820-1834.
- Cowles, J., Boldgiv, B., Liancourt, P., Petraitis, P. S., & Casper, B. B. (2018). Effects of increased temperature on plant communities depend on landscape location and precipitation. *Ecology and evolution*, 8(11), 5267-5278.
- Crauss, A. (2018). River Fire 100% contained, but over 12,500 firefighters still battling California fires. *KRCR News Channel*. <https://krcrtv.com/north-coast-news/eureka-local-news/river-fire-100-contained-but-over-12500-firefighters-still-battling-california-fires>

- Crippen, R. E. (1990). Calculating the vegetation index faster. *Remote sensing of Environment*, 34(1), 71-73.
- Cumming, S. G. (2005). Effective fire suppression in boreal forests. *Canadian Journal of Forest Research*, 35(4), 772-786.
- Dai, A. (2013). Increasing drought under global warming in observations and models. *Nature climate change*, 3(1), 52.
- Delfino, R., Brummel, S., Wu, J., Stern, H., Ostro, B., Lipsett, M., Winer, A., Street, D.H., Zhang, L., Tioa, T. and Gillen, D. (2009). The Relationship of Respiratory and Cardiovascular Hospital Admissions to the Southern California Wildfires of 2003. *Occupational and Environmental Medicine*, 66, 189-197.
- Dessler, A. E., Zhang, Z., & Yang, P. (2008). Water-vapor climate feedback inferred from climate fluctuations, 2003–2008. *Geophysical Research Letters*, 35(20).
- Dickson, P. (2001). *Sputnik: The shock of the century*. Bloomsbury Publishing USA.
- Dokas, I., Statheropoulos, M., & Karma, S. (2007). Integration of field chemical data in initial risk assessment of forest fire smoke. *Science of the total environment*, 376(1-3), 72-85.
- Dozier, J. (1981) A method for satellite identification of surface temperature fields of subpixel resolution. *Remote Sens. Environ.* 11, 221–229.
- Environment and Climate Change Canada (2017). Canadian Environmental Sustainability Indicators. *Greenhouse Gas Emissions*.
- Flannigan, M., Stocks, B., Turetsky, M., & Wotton, M. (2009). Impacts of climate change on fire activity and fire management in the circumboreal forest. *Global Change Biology*, 15(3), 549-560.

- Flannigan, M., Cantin, A. S., De Groot, W. J., Wotton, M., Newbery, A., & Gowman, L. M. (2013). Global wildland fire season severity in the 21st century. *Forest Ecology and Management*, 294, 54-61.
- Fowler, C. T. (2003). Human health impacts of forest fires in the southern United States: a literature review. *Journal of Ecological Anthropology*, 7(1), 39-63.
- Funk, C. C., & Brown, M. E. (2006). Intra-seasonal NDVI change projections in semi-arid Africa. *Remote Sensing of Environment*, 101(2), 249-256.
- Gates, David M. (1980). *Biophysical Ecology*, Springer-Verlag, New York, 611 p
- Girardin, M. P., & Wotton, B. M. (2009). Summer moisture and wildfire risks across Canada. *Journal of Applied Meteorology and Climatology*, 48(3), 517-533.
- Haikerwal A, et al. (2016) Fine particulate matter (PM_{2.5}) exposure during a prolonged wildfire period and emergency department visits for asthma. *Respirology* 21: 88–94.
- Hansen, J., Ruedy, R., Sato, M., & Lo, K. (2010). Global surface temperature change. *Reviews of Geophysics*, 48(4).
- Herold, M., Mayaux, P., Woodcock, C. E., Baccini, A., & Schmullius, C. (2008). Some challenges in global land cover mapping: An assessment of agreement and accuracy in existing 1 km datasets. *Remote Sensing of Environment*, 112(5), 2538-2556.
- Harris Geospatial Solutions (2020). E0-1 Hyperion Vegetation Indices Tutorial. *L3HARRIS Geospatial Solutions*. <https://www.harrisgeospatial.com/docs/ForestHealthTool.html>
- Harvey, B. J. (2016). Human-caused climate change is now a key driver of forest fire activity in the western United States. *Proc Natl Acad Sci USA* 113:11649–11650.
- Haynes, W. M. (2011). *CRC handbook of chemistry and physics*. CRC press. p. 10.233. ISBN 978-1-4398-5511-9.

- Hendry GAF, Houghton JD, Brown SB (1987). The degradation of chlorophyll – A biological enigma. *New Phytol* 107: 255-302.
- Hinkley, E.A.; Zajkowski, T. (2011). USDA forest service-NASA: Unmanned aerial systems demonstrations-pushing the leading edge in fire mapping. *Geocarto Int.* 26, 103–111.
- Hirsch, K. G., Corey, P. N., & Martell, D. L. (1998). Using expert judgment to model initial attack fire crew effectiveness. *Forest Science*, 44(4), 539-549.
- Hogue, C. (2005). No vote for US in chemicals treaty. *Chemical and Engineering News*, 83, 26-27.
- Jaffe D, Hafner W, Chand D, Westerling A, Spracklen D (2008) Interannual variations in PM_{2.5} due to wildfires in the Western United States. *Environ Sci Technol* 42: 2812–2818.
- Jain, T. B., Graham, R. T., & Pilliod, D. S. (2004). Tongue-tied: confused meanings for common fire terminology can lead to fuels mismanagement. *Wildfire. July/August: 22-26.*, 22-26.
- Joby, N. E., George, N. S., & Geethasree, M. N. (2019). Storm tracking using Geo-stationary lightning observation videos.
- Jollineau, M. Y., & Howarth, P. J. (2008). Mapping an inland wetland complex using hyperspectral imagery. *International Journal of Remote Sensing*, 29(12), 3609-3631.
- Joseph, S., Murthy, M. S. R., & Thomas, A. P. (2011). The progress on remote sensing technology in identifying tropical forest degradation: a synthesis of the present knowledge and future perspectives. *Environmental Earth Sciences*, 64(3), 731-741.
- Knee, M. (1972). Anthocyanin, carotenoid, and chlorophyll changes in the peel of Cox's Orange Pippin apples during ripening on and off the tree. *Journal of experimental botany*, 184-196.

- Knee, M. (1988). Carotenol esters in developing apple fruits. *Phytochemistry*, 27(4), 1005-1009.
- Koetz, B., Morsdorf, F., Van der Linden, S., Curt, T., & Allgöwer, B. (2008). Multi-source land cover classification for forest fire management based on imaging spectrometry and LiDAR data. *Forest Ecology and Management*, 256(3), 263-271.
- Kokaly, R. F., Rockwell, B. W., Haire, S. L., & King, T. V. (2007). Characterization of post-fire surface cover, soils, and burn severity at the Cerro Grande Fire, New Mexico, using hyperspectral and multispectral remote sensing. *Remote Sensing of Environment*, 106(3), 305-325.
- Kontoes, C.; Keramitsoglou, I.; Sifakis, N.; Konstantinidis, P. (2009). SITHON: An Airborne Fire Detection System Compliant with Operational Tactical Requirements. *Sensors* 2009, 9, 1204–1220.
- Kourtz, P. (1987). The need for improved forest fire detection. *The Forestry Chronicle*, 63(4), 272-277.
- Kourtz, P. H. (1994). Advanced information systems in Canadian forest fire control.
- Kuenzer, C.; Dech, S. (2013). Theoretical Background of Thermal Infrared Remote Sensing. In *Thermal Infrared Remote Sensing*; Kuenzer, C., Dech, S., Eds.; Springer: Dordrecht, The Netherlands, 2013; Volume 17, pp. 1–26
- Larson, T. V., & Koenig, J. Q. (1994). Wood smoke: emissions and noncancer respiratory effects. *Annual review of public health*, 15(1), 133-156.
- Langmann, B., Duncan, B., Textor, C., Trentmann, J., & van der Werf, G. R. (2009). Vegetation fire emissions and their impact on air pollution and climate. *Atmospheric environment*, 43(1), 107-116.

- Leblon, B., Bourgeau-Chavez, L., & San-Miguel-Ayanz, J. (2012). Use of remote sensing in wildfire management. *Sustainable development-authoritative and leading edge content for environmental management*, 55-81.
- Liew, S. C. (2017). *Electromagnetic Waves*. Centre for Remote Imaging, Sensing and Processing.
- Lin, J. C., Matsui, T., Pielke Sr, R. A., & Kummerow, C. (2006). Effects of biomass-burning-derived aerosols on precipitation and clouds in the Amazon Basin: A satellite-based empirical study. *Journal of Geophysical Research: Atmospheres*, 111(D19).
- Liu, Z., Murphy, J. P., Maghirang, R., & Devlin, D. (2016). Health and environmental impacts of smoke from vegetation fires: a review. *Journal of Environmental Protection*, 7, 1860-1885.
- Lo, C. P. (1986). *Applied remote sensing*. Taylor & Francis, 60.
- Lydersen, J. M., North, M. P., & Collins, B. M. (2014). Severity of an uncharacteristically large wildfire, the Rim Fire, in forests with relatively restored frequent fire regimes. *Forest Ecology and Management*, 328, 326-334.
- Lyon, J. G., Yuan, D., Lunetta, R. S., & Elvidge, C. D. (1998). A change detection experiment using vegetation indices. *Photogrammetric engineering and remote sensing*, 64(2), 143-150.
- Martell, D. L., & Sun, H. (2008). The impact of fire suppression, vegetation, and weather on the area burned by lightning-caused forest fires in Ontario. *Canadian Journal of Forest Research*, 38(6), 1547-1563.
- Matile, P., Flach, B. M. P., & Eller, B. M. (1992). Autumn leaves of *Ginkgo biloba* L.: optical properties, pigments and optical brighteners. *Botanica acta*, 105(1), 13-17.

- Matson, M., & Dozier, J. (1981). Identification of subresolution high temperature sources using a thermal IR sensor. *Photogrammetric Engineering and Remote Sensing*, 47(9), 1311-1318.
- McClure, C. D., & Jaffe, D. A. (2018). US particulate matter air quality improves except in wildland fire-prone areas. *Proceedings of the National Academy of Sciences*, 115(31), 7901-7906.
- McDonald, F., & Naugle, J. E. (2008). Discovering Earth's Radiation Belts: Remembering Explorer 1 and 3. *Eos, Transactions American Geophysical Union*, 89(39), 361-363.
- McFayden, C. B., Woolford, D. G., Stacey, A., Boychuk, D., Johnston, J. M., Wheatley, M. J., & Martell, D. L. (2019). Risk assessment for wildland fire aerial detection patrol route planning in Ontario, Canada. *International Journal of Wildland Fire*.
- McFayden, C. B., Woolford, D. G., Stacey, A., Boychuk, D., Johnston, J. M., Wheatley, M. J., & Martell, D. L. (2020). Risk assessment for wildland fire aerial detection patrol route planning in Ontario, Canada. *International Journal of Wildland Fire*, 29(1), 28-41.
- McHugh, D., & Gil, J. (2018). Senescence and aging: causes, consequences, and therapeutic avenues. *J Cell Biol*, 217(1), 65-77.
- McMahon, C. K., and Bush, P. B. (1992). Forest worker exposure to airborne herbicide residues in smoke from prescribed fires in the southern United States. *Am. Ind. Hyg. Assoc.* 53(4):265-272.
- Merino, L.; Caballero, F.; Martínez-de Dios, Jr.; Ferruz, J.; Ollero, A. (2006). A cooperative perception system for multiple UAVs: Application to automatic detection of forest fires. *J. Field Robot.* 23, 165-184.

- Merzlyak, M. N., Gitelson, A. A., Chivkunova, O. B., & Rakitin, V. Y. (1999). Non-destructive optical detection of pigment changes during leaf senescence and fruit ripening. *Physiologia plantarum*, 106(1), 135-141.
- Ministry of the Environment, Conservation and Parks (MECP). (2016). *Daisy Lake Uplands Provincial Park Management Statement*. Retrieved from the Ontario Government website: <https://www.ontario.ca/page/daisy-lake-uplands-provincial-park-management-statement>
- Ministry of Natural Resources and Forestry of Canada (MNRFC). (2017). *Forest Fire Management*. Retrieved from the Ontario Government website: <https://www.ontario.ca/page/forest-fire-management>
- Ministry of Natural Resources and Forestry of Canada (MNRFC). (2018). *Forest Fires; Fires: year to date*. Retrieved from the Ontario Government website: <https://www.ontario.ca/page/forest-fires>
- Miranda, A. I., and Borrego, C. 2005. Effects on health from forest fire smoke. *Forest Fire Net* 3:16
- Mukerjee, D. (1998). Health impact of polychlorinated dibenzo-p-dioxins: a critical review. *Journal of the air & waste management association*, 48(2), 157-165.
- NAAQS. (2016). *United states environmental protection agency; NAAQS Table*. Retrieved from: <https://www.epa.gov/criteria-air-pollutants/naaqs-table>
- Naeher, L. P., Brauer, M., Lipsett, M., Zelikoff, J. T., Simpson, C. D., Koenig, J. Q., and Smith, K. R. (2007). Woodsmoke health effects, a review. *Inhal. Toxicol.* 19(1):67–106.
- Nav Canada (2019). Canada Flight Supplement. Effective 0901Z 20 June 2019 to 0901Z 15 August 2019

- Njoku, E. G., & Entekhabi, D. (1996). Passive microwave remote sensing of soil moisture. *Journal of hydrology*, 184(1-2), 101-129.
- Natural Resources Canada (2016). (NRC, 2016). Daisy Lake. <http://www4.rncan.gc.ca/search-place-names/unique.php?id=FAVEN&output=xml>
- Nelson, G. L. (1987). Regulatory aspects of fire toxicology. *Toxicology* 47(1-2):181-199.
- Ollero, A., Arrúe, B. C., Martínez, J. R., & Murillo, J. J. (1997). False alarm reduction components for infrared detection of forest fires. *IFAC Proceedings Volumes*, 30(7), 275-280.
- Ollero, A., Arrue, B. C., Martínez, J. R., & Murillo, J. J. (1999). Techniques for reducing false alarms in infrared forest-fire automatic detection systems. *Control Engineering Practice*, 7(1), 123-131.
- Ollero, A., & Merino, L. (2006). Unmanned aerial vehicles as tools for forest-fire fighting. *Forest Ecology and Management*, 234(1), S263.
- Ozyavuz, M., Bilgili, B. C., & Salici, A. (2015). Determination of vegetation changes with NDVI method. *Journal of Environmental Protection and Ecology*, 16(1), 264-273.
- Pannkuk, C. D., & Robichaud, P. R. (2003). Effectiveness of needle cast at reducing erosion after forest fires. *Water Resources Research*, 39(12).
- Pappas, C., Matheny, A. M., Baltzer, J. L., Barr, A. G., Black, T. A., Bohrer, G., ... & Stephens, J. (2018). Boreal tree hydrodynamics: asynchronous, diverging, yet complementary. *Tree physiology*, 38(7), 953-964.
- Penížek, V., Zádorová, T., Kodešová, R., & Vaněk, A. (2016). Influence of elevation data resolution on spatial prediction of colluvial soils in a Luvisol region. *PloS one*, 11(11), e0165699.

- Peterson, D. A., Hyer, E. J., Campbell, J. R., Fromm, M. D., Hair, J. W., Butler, C. F., & Fenn, M. A. (2015). The 2013 Rim Fire: Implications for predicting extreme fire spread, pyroconvection, and smoke emissions. *Bulletin of the American Meteorological Society*, 96(2), 229-247.
- Polivka, T. N., Wang, J., Ellison, L. T., Hyer, E. J., & Ichoku, C. M. (2016). Improving nocturnal fire detection with the VIIRS day–night band. *IEEE Transactions on Geoscience and Remote Sensing*, 54(9), 5503-5519.
- Rittmaster, R., Adamowicz, W. L., Amiro, B., & Pelletier, R. T. (2006). Economic analysis of health effects from forest fires. *Canadian Journal of Forest Research*, 36(4), 868-877.
- Robert, A. S. (2007). Remote sensing: Models and methods for image processing. *By Elsevier Inc.* p300-304.
- Robinson, J. M. (1991). Fire from space: Global fire evaluation using infrared remote sensing. *International Journal of Remote Sensing*, 12(1), 3-24.
- Rocha, V., & Xia, R. (2014). Man arrested on suspicion of arson in out-of-control King fire. *Los Angeles Times*. <https://www.latimes.com/local/la-me-ln-arson-arrest-king-fire-northern-california-20140918-story.html>
- Rodriguez-Galiano, V. F., Ghimire, B., Rogan, J., Chica-Olmo, M., & Rigol-Sanchez, J. P. (2012). An assessment of the effectiveness of a random forest classifier for land-cover classification. *ISPRS Journal of Photogrammetry and Remote Sensing*, 67, 93-104.
- Rouse, J. W., Haas, R. H., Schell, J. A., & Deering, D. W. (1974). Monitoring vegetation systems in the Great Plains with ERTS. *NASA special publication*, 351, 309.

- Safe, S. H. (1986). Comparative toxicology and mechanism of action of polychlorinated dibenzo-p-dioxins and dibenzofurans. *Annual review of pharmacology and toxicology*, 26(1), 371-399.
- Schroeder, M. J., & Buck, C. C. (1970). Fire weather: a guide for application of meteorological information to forest fire control operations. *The Bark Beetles, Fuels, and Fire Bibliography*, 14.
- Shippert, P. (2004). Why use hyperspectral imagery?. *Photogrammetric engineering and remote sensing*, 70(4), 377-396.
- Simoneit, B. R. (2002). Biomass burning—a review of organic tracers for smoke from incomplete combustion. *Applied Geochemistry*, 17(3), 129-162.
- Staley, D. M. (2013). Emergency assessment of post-fire debris-flow hazards for the 2013 Rim Fire, Stanislaus National Forest and Yosemite National Park, California. *US Geological Survey Open-File Report*, 1260(11).
- Statheropoulos, M., & Goldammer, J. G. (2007, May). Vegetation fire smoke: Nature, impacts and policies to reduce negative consequences on humans and the environment. In *A Publication of the Council of Europe as a contribution to the 4th International Wildland Fire Conference. Sevilla, Spain* (pp. 13-17).
- Stavros, E.N., Z. Tane, V. Kane, S. Veraverbeke, R. McGaughey, J.A. Lutz, C. Ramirez, and D.S. Schimel. (2016). Remote Sensing Data Before and After California Rim and King Forest Fires, 2010-2015. ORNL DAAC, Oak Ridge, Tennessee, USA.
<https://doi.org/10.3334/ORNLDAAC/1288>

- Stavros, E. N., Coen, J., Peterson, B., Singh, H., Kennedy, K., Ramirez, C., & Schimel, D. (2018). Use of imaging spectroscopy and LIDAR to characterize fuels for fire behavior prediction. *Remote Sensing Applications: Society and Environment*, 11, 41-50.
- Stefanidou, M., Athanaselis, S., & Spiliopoulou, C. (2008). Health impacts of fire smoke inhalation. *Inhalation toxicology*, 20(8), 761-766.
- Stokes, A., Douglas, G. B., Fourcaud, T., Giadrossich, F., Gillies, C., Hubble, T., ... & Mickovski, S. B. (2014). Ecological mitigation of hillslope instability: ten key issues facing researchers and practitioners. *Plant and Soil*, 377(1-2), 1-23.
- Tan, W. C., Qiu, D., Liam, B. L., NG, T. P., Lee, S. H., van Eeden, S. F., ... & Hogg, J. C. (2000). The human bone marrow response to acute air pollution caused by forest fires. *American journal of respiratory and critical care medicine*, 161(4), 1213-1217.
- Thenkabail, P. S., Enclona, E. A., Ashton, M. S., & Van Der Meer, B. (2004). Accuracy assessments of hyperspectral waveband performance for vegetation analysis applications. *Remote sensing of environment*, 91(3-4), 354-376.
- Thenkabail, P. S., & Lyon, J. G. (Eds.). (2016). *Hyperspectral remote sensing of vegetation*. CRC press.
- Townsend, P. A., & Foster, J. R. (2002, June). Comparison of EO-1 Hyperion to AVIRIS for mapping forest composition in the Appalachian Mountains, USA. In *IEEE International Geoscience and Remote Sensing Symposium* (Vol. 2, pp. 793-795). IEEE.
- Tran, Q. H., Han, D., Kang, C., Haldar, A., & Huh, J. (2017). Effects of ambient temperature and relative humidity on subsurface defect detection in concrete structures by active thermal imaging. *Sensors*, 17(8), 1718.

- Trenberth, K. E., Dai, A., Rasmussen, R. M., & Parsons, D. B. (2003). The changing character of precipitation. *Bulletin of the American Meteorological Society*, 84(9), 1205-1218.
- Tyo, J. S., Goldstein, D. L., Chenault, D. B., & Shaw, J. A. (2006). Review of passive imaging polarimetry for remote sensing applications. *Applied optics*, 45(22), 5453-5469.
- Ullah, I., Baharom, M. N. R., Ahmad, H., Wahid, F., Luqman, H. M., Zainal, Z., & Das, B. (2019). Smart lightning detection system for smart-city infrastructure using artificial neural network. *Wireless Personal Communications*, 106(4), 1743-1766.
- USDA (2003). California Department of Forestry and Fire Protection and Forest Service Department of Agriculture. *The 2003 San Diego County Fire Siege Fire Safety Review*. https://www.fs.usda.gov/Internet/FSE_DOCUMENTS/stelprdb5297020.pdf
- USDA (2013). California Department of Forestry and Fire Protection and Forest Service Department of Agriculture. *RIM FIRE- Preliminary Fuel Treatment Effectiveness Report*. https://www.fs.usda.gov/Internet/FSE_DOCUMENTS/stelprdb5436551.pdf
- Van Wagner, C. E. (1974). *Structure of the Canadian forest fire weather index* (Vol. 1333). Environment Canada, Forestry Service.
- Veraverbeke, S., Dennison, P., Gitas, I., Hulley, G., Kalashnikova, O., Katagis, T., ... & Stavros, N. (2018). Hyperspectral remote sensing of fire: State-of-the-art and future perspectives. *Remote Sensing of Environment*, 216, 105-121.
- Vestin, A., Rissler, J., Swietlicki, E., Frank, G. P., & Andreae, M. O. (2007). Cloud-nucleating properties of the Amazonian biomass burning aerosol: Cloud condensation nuclei measurements and modeling. *Journal of Geophysical Research: Atmospheres*, 112(D14).
- Villars, F., & Weisskopf, V. F. (1954). The scattering of electromagnetic waves by turbulent atmospheric fluctuations. *Physical Review*, 94(2), 232.

- Vogelmann, J. E., & Rock, B. N. (1985). Spectral characterization of suspected acid deposition damage in red spruce (*Picea Rubens*) stands from Vermont.
- Wegesser, T. C., Pinkerton, K. E., & Last, J. A. (2009). California wildland fires of 2008: coarse and fine particulate matter toxicity. *Environmental health perspectives*, 117(6), 893.
- Westerling AL, Hidalgo HG, Cayan DR, Swetnam TW (2006). Warming and earlier spring increase western U.S. forest wildfire activity. *Science* 313:940–943
- World Health Organization. 1999. Health guidelines for vegetation fire events, Lima, Peru, 6–9 October 1998.
- Woolford, D. G., Dean, C. B., Martell, D. L., Cao, J., & Wotton, B. M. (2014). Lightning-caused forest fire risk in Northwestern Ontario, Canada, is increasing and associated with anomalies in fire weather. *Environmetrics*, 25(6), 406–416.
- Wooster, M.J.; Roberts, G.; Smith, A.M.S.; Johnston, J.; Freeborn, P.; Amici, S.; Hudak, A.T. (2013). Thermal Remote Sensing of Active Vegetation Fires and Biomass Burning Events. In *Thermal Infrared Remote Sensing*; Kuenzer, C., Dech, S., Eds.; Springer: Dordrecht, The Netherlands, 2013; Volume 17, pp. 347–390.
- Wotton, B. M., & Martell, D. L. (2005). A lightning fire occurrence model for Ontario. *Canadian Journal of Forest Research*, 35(6), 1389–1401.
- Yuan, C., Zhang, Y., & Liu, Z. (2015). A survey on technologies for automatic forest fire monitoring, detection, and fighting using unmanned aerial vehicles and remote sensing techniques. *Canadian journal of forest research*, 45(7), 783–792.
- Zimmerman, E.W. (1969). *Forest Fire Detection*; U.S. Department of Agriculture: Washington, DC, USA, 1969.